


ESTIMATION OF SOIL MOISTURE IN THE SOUTHERN UNITED STATES IN 2003
USING MULTI-SATELLITE REMOTE SENSING MEASUREMENTS


by

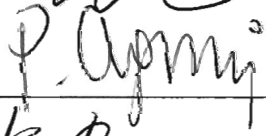
Melissa Soriano
A Thesis
Submitted to the
Graduate Faculty
of
George Mason University
in Partial Fulfillment of
The Requirements for the Degree
of
Master of Science
Earth System Science

Committee:


_____ Dr. John Qu, Thesis Director


_____ Dr. Ruixin Yang, Committee Member


_____ Dr. Sheryl Beach, Committee Member


_____ Dr. Peggy Agouris,
Department Chairperson


_____ Dr. Peter Becker, Associate Dean
for Graduate Programs, College
of Science


_____ Dr. Vikas Chandhoke, Dean,
College of Science

Date: Nov. 24, 2008 _____ Fall Semester 2008
George Mason University
Fairfax, VA

Estimation of Soil Moisture in the Southern United States in 2003 Using Multi-Satellite
Remote Sensing Measurements

A thesis submitted in partial fulfillment of the requirements for the degree of Master of
Science at George Mason University

By

Melissa Soriano
Bachelors of Science
California Institute of Technology, 2003

Director: Dr. John Qu, Associate Professor
Department of Geography and Geoinformation Science

Fall Semester 2008
George Mason University
Fairfax, VA

Copyright: 2008 Melissa Soriano
All Rights Reserved

DEDICATION

This is dedicated to my family.

ACKNOWLEDGEMENTS

First and foremost, I would like to thank my advisor, Dr. John Qu, Co-Director of EastFIRE Lab, for his guidance, advice, and words of motivation and encouragement when I needed them most. This thesis would not be possible without him. I look forward to a lifelong collaboration. Thank you to Dr. Xianjun Hao, also of the EastFIRE lab, for his technical advice and insight regarding the MODIS Level 1 data processing. Thank you to Dr. Lingli Wang for blazing the trail with her work on soil moisture using MODIS data. Thank you to George Mason University for giving me the opportunity to pursue work that I love. Thank you to Dr. William Teng of the GES DISC for his advice and support. Dr. Teng was the architect of the AERS PGE. His words of wisdom and tales of graduate school at Cornell convinced me that I could do it too. Thank you also to Dr. Patrick Starks of the USDA ARS for providing the Berg station data which this study uses extensively. Thank you to Andre Jongeling and Robert Navarro of the Jet Propulsion Laboratory for allowing me to take an educational leave of absence and welcoming me back when I finished my classes.

Thank you to my father, Arturo, for being my constant inspiration. Thank you to my mother, who couldn't be here but whose presence will always be with me, lighting the fire inside me, and motivating me to always be the best person I can be. I hope she would be proud of me. Thank you to all my family for their unconditional support and love throughout graduate school, especially Natalie, Dominick, Losha, Linda, and Danielle. I never thought I'd be here but I am! I can only imagine what will be next.

TABLE OF CONTENTS

	Page
List of Tables.....	vi
List of Figures.....	vii
Abstract.....	viii
Introduction.....	1
Literature Review.....	6
Theory.....	18
Study Areas	23
Data Sources.....	26
Methodology.....	37
Results 42	
Conclusion and Discussion.....	53
List of References.....	58

LIST OF TABLES

Table	Page
Table 1- USDA Soil Classification System.....	3
Table 2- Passive Microwave Sensing Instruments Used to Measure Soil Moisture.....	6
Table 3- AMSR-E Sensor Specifications.....	9
Table 4- Microwave Temperature of Three Representative Types of Material.....	18
Table 5- AMSR-E ATBD Model terms and Definitions.....	21
Table 6- Radiative Transfer Equation Contributing Factors.....	22
Table 7- Technical Specifications of Stevens-Vitel Hydra Probe.....	27
Table 8- ARS Micronet Station Information.....	30
Table 9- MODIS Product Names and Descriptions.....	35
Table 10- Major U.S. field campaigns using airborne microwave instruments.....	36
Table 11- Satellite Bounding Box Coordinates containing Berg Micronet Station.....	37
Table 12- Correlation between AMSR-E soil moisture and in-situ measurements at LWREW in 2003.....	44
Table 13- Correlation between TMI soil moisture and in-situ measurements at LWREW in 2003.....	44
Table 14- Correlation between AMSR-E soil moisture and in-situ measurements at LREW in 2003.....	48
Table 15- Correlation between TMI soil moisture and in-situ measurements at LREW in 2003.....	48
Table 16- Criteria for valid MODIS daily data.....	49

LIST OF FIGURES

Figure	Page
Figure 1- Proportions of sand, silt, and clay in the basic soil textural classes.....	4
Figure 2- Variations in dielectric constant as a function of soil moisture.....	19
Figure 3- Model Representation of a Spaceborne Radiometer Viewing a Heterogeneous Earth.....	21
Figure 4- Little Washita Experimental Watershed.....	24
Figure 5- Little Washita Soil Moisture June 2003.....	42
Figure 6- Little Washita Soil Moisture July 2003.....	43
Figure 7- Little Washita Soil Moisture August 2003.....	43
Figure 8- Little Washita Ground and Satellite Soil Moisture, June-August 2003.....	44
Figure 9- Little River Soil Moisture June 2003.....	45
Figure 10- Little River Soil Moisture July 2003.....	45
Figure 11- Little River Soil Moisture August 2003.....	46
Figure 12- Little River Soil Moisture December 2003.....	46
Figure 13- Little River Soil Moisture January 2003.....	47
Figure 14- Little River Soil Moisture February 2003.....	47
Figure 15- Correlation of Calculated Soil Moisture using MODIS Data with Measured Soil Moisture for June – August of 2003.....	50

ABSTRACT

ESTIMATION OF SOIL MOISTURE IN THE SOUTHERN UNITED STATES IN 2003 USING MULTI-SATELLITE REMOTE SENSING MEASUREMENTS

Melissa Soriano, MS

George Mason University, 2008

Thesis Director: Dr. John Qu

Soil moisture is a critical parameter for predicting and detecting floods and droughts, as well as indicating crop and vegetation health. Current indicators utilize surrogate or modeled measures of soil moisture. Actual observed soil moisture measurements have the potential to improve understanding of floods, droughts, and crop health.

In this study, ground soil moisture daily average values were compared to estimates obtained from two microwave sensors, the EOS Aqua Advanced Microwave Scanning Radiometer (AMSR-E) and the Tropical Rainfall Measurement Mission Microwave Scanning Radiometer (TMI), as well as one optical sensor, the EOS Aqua Moderate Resolution Imaging Spectroradiometer (MODIS). The study areas were the Little Washita River Experimental Watershed in Oklahoma and the Little River Experimental Watershed in Georgia. This research compared AMSR-E, TMI, and MODIS data to ground data from the Little Washita Berg station and also compared

AMSR-E and TMI data to ground data from the Little River Soil Climate Analysis Network station.

AMSR-E and TMI performed better in Little Washita than in Little River during the crop-covered season. This may be due to the vegetation type, distribution, and density at Little River. AMSR-E exhibited a smaller range of variability than the TMI or in-situ measurements at both study sites for all time periods. In the crop-covered season of June, July, and August of 2003, MODIS soil moisture retrieval at the Little Washita site correlated better ($R^2 = 0.772$) with the in-situ measurements than AMSR-E or TMI soil moisture retrievals. The spatial resolution of MODIS (1 km) is finer than the spatial resolution of AMSR-E (~25 km) or TMI. Spatial resolution is an important factor because topography, soil properties, and vegetation cover may vary significantly over satellite footprints. Both microwave sensors are limited by their coarse spatial resolution. However, optical measurements are limited to cloud-free conditions. Future work includes research on algorithms which combine optical and microwave measurements to provide the advantages of each.

INTRODUCTION

Soil moisture is a crucial component of land surface hydrology. Precipitation, soil moisture storage (infiltration), evapotranspiration, surface runoff, and groundwater flow compose the hydrologic cycle [Dzurik, 2003]. Soil moisture has a dominant influence on runoff [Merz and Plate, 1997] and is therefore valuable in predicting floods. Soil moisture is also important for maintaining crop and vegetation health [Doraiswamy *et al*, 2004]. Measured changes in soil moisture can be used to optimize irrigation scheduling and crop water use to maximize agricultural yield [Bailey and Spackman, 2007]. Observed soil moisture content is also significantly correlated to the Palmer Drought Severity Index, the most prominent index of meteorological drought in the United States [Dai *et al*, 2004]. Monitoring soil moisture offers the possibility of detecting and predicting drought.

A few surrogate measures of soil moisture exist, such as Antecedent Precipitation Index (API), flood index, and crop index. For example, Teng *et al* compared brightness temperatures from the Special Sensor Microwave/Imager (SSM/I) to API over the U.S. Corn Belts from 1987 to 1990 and found a good correlation over semi-arid regions [Teng *et al*, 1993]. However the API model makes several critical assumptions about the behavior of soil moisture with respect to precipitation. The model depends on initial conditions (or soil moisture). Compared to API, soil moisture is a better predictor of

future monthly temperature [*Huang et al, 1996*]. Direct soil moisture measurements have the potential to improve hydrologic models.

Remote sensing has shown great promise in providing improved spatial and temporal coverage of soil moisture measurements [*Wagner et al, 2006*]. Although many studies have analyzed microwave soil moisture observations and compared them to in-situ measurements, most of these studies have been limited to a single region or the short time period of a field campaign due to a lack of comprehensive ground data. This study aims to characterize and compare surface soil moisture measurements made from multiple satellites (AMSR-E, TMI, MODIS) with in-situ soil moisture values over two watersheds located in the Southern United States over the span of a year. This study's goal is not validation. As Anderson and Bates state, "model validation in an absolute sense is not possible" [*Anderson and Bates, 2001*]. Evaluating remote sensing models used in hydrology is complicated by the scaling issues inherent in comparing a satellite measurement which is the spatial average over the horizontal footprint and vertical sampling depth with a limited set of field observations made at single points. Nevertheless, characterization and comparison of these data sets is useful in improving understanding of satellite measurement of soil moisture.

Soil consists of four major components: inorganic (mineral) materials, organic matter, water, and air. These components cluster, forming particles. A representative soil which is well-suited for plant growth is typically made up of about 50% pore space. These pores may be filled with air and/or water. Two important properties of soils are texture and structure. Soil texture describes the relative proportions of different size

particles while soil structure defines their arrangements into groups. A soil's texture is a basic property that will not change. The U.S. Department of Agriculture classifies soil particles into four main categories by size. This classification system is described in Table 1. The largest particles are classified as gravel, followed by sand, silt, and lastly clay [Schaetzl and Anderson, 2005].

Table 1- USDA Soil Classification System

Type of Particle	Clay	Silt	Sand	Gravel
Size	< 0.002 mm	0.002-0.05 mm	0.05-2.0 mm	> 2 mm

Sand and gravel are large enough to be distinguishable as separate particles. Sandy soil contains large pores that are few in size, resulting in a low ability to store soil moisture and high infiltration rates. Sandy soils encourage movement of air and water. Sand and silt are typically composed mostly of quartz, as well as primary silicates such as feldspars, hornblende, and micas. In contrast, clay particles have many more pores of a smaller size. Clay particles have the most surface area. A particle of fine clay can have 10,000 times more surface area than the same weight of sand. As adsorption of water, nutrients and gas is accomplished at the particle's surface, clay has excellent adsorption power and cohesion. Clay particles are therefore efficient in soil moisture storage and have the lowest infiltration rates of all the particles. Clay particles are dominated by secondary silicates [Brady, 1974].

Particles are classified through the use of multiple sieves. Soil samples are broken up and suspended in water, where they tend to sink and settle, passing through the sieve if they are small enough. The percentage of particles of each size is determined and

used to classify the soil into textural classes using the texture triangle system shown in Figure 1. The main soil textural classes are sands, loams, and clays. Sands by definition are composed of at least 70% sand particles. Clays are made up of at least 35-40% clay particles. Loams are mixtures of sand, silt, and clay and therefore have qualities of small and large particles. Loams which are dominated by sand are sandy loam; likewise there are silt loams and clay loams [Lal and Shukla, 2004].

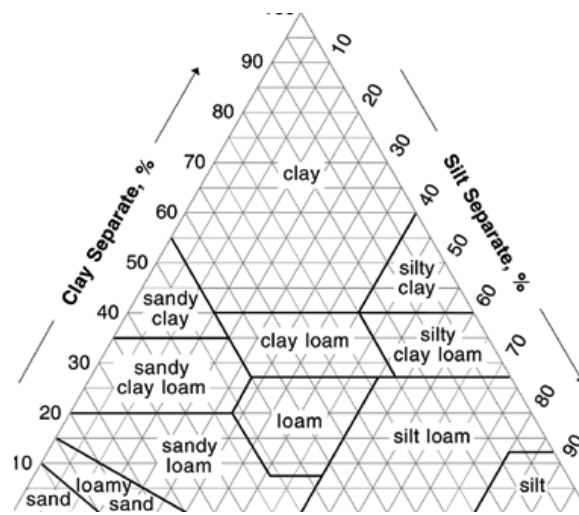


Figure 1- Proportions of sand, silt, and clay in the basic soil textural classes (Source: USDA Soil Survey Manual, 1993)

Soil formation is influenced by climate (especially precipitation and air temperature), living organisms, the nature of the parent material, and the topography of the region. Over time, distinct layers, or horizons form. The sequences of horizons which exist in a particular soil define the soil profile. Five general categories of horizons exist: O (organic), A (eluvial), B (illuvial), C, and R. The O layer forms at the top of most soils. It is composed of litter from dead plants and animals. In the O1 layer, the original forms of these substances can be recognized with the naked eye, whereas in the

O₂ layer, it cannot. The organic material in the O layers provides enriching nutrients for the soil such as nitrogen and potassium. The A layer is characterized by the zone of maximum eluviation, the leaching of minerals by the soil that is driven by the downwards movement of water. In the A layers, organic matter mixes with inorganic materials. The B layer is characterized by illuviation, the upwards movement of minerals which occurs as plants obtain water from the soil. The C layer is the weathered parent material which is deep enough that it is not significantly influenced by major biological activities. The R layer is bedrock [*Ashman and Puri, 2002*].

LITERATURE REVIEW

A partial list of current and past passive *microwave* satellite missions is shown in Table 2. Each satellite's temporal and spatial coverage is described, as well as the useful frequencies available for remote sensing of soil moisture. Earlier missions which are not shown include NASA's Nimbus 5 and 6 (1972-1978), NOAA's Microwave Sounding Unit (1978-1998), and NOAA's Advanced Microwave Sounding Unit (1998-) [Grody *et al*, 2000].

**Table 2- Passive Microwave Remote Sensing Instruments
Used to Measure Soil Moisture**

Mission/Instrument	Temporal coverage	Spatial Resolution	Frequencies
Nimbus-7 Scanning Multi-channel Microwave Radiometer (SMMR)	October 1978 to August 1987	25 km	6.6 GHz
Defense Meteorological Satellite Program Special Sensor Microwave Imager (SSM/I)	1987 to Present	43 x 69 km	19.3 GHz
Aqua Advanced Microwave Scanning Radiometer (AMSR-E)	Daily, 2002-present	$\frac{1}{4}^{\circ}$ (~25 km)	6.9 GHz, 10.7 GHz
Advanced Earth Observing Satellite II (ADEOS-II) AMSR	Daily, 2002-present	$\frac{1}{4}^{\circ}$ (~25 km)	6.9 GHz, 10.7 GHz
Tropical Rainfall Measuring Mission (TRMM) Microwave Imager (TMI)	Daily, 2002-present	$\frac{1}{8}^{\circ}$	10.65 GHz

The Scanning Multi-channel Microwave Radiometer (SMMR) was the first satellite to demonstrate success in retrieving soil moisture using a microwave radiometer. Soil moisture measurements from SMMR were compared to in-situ data from 79 sites in

the former Soviet Union. No ancillary data were available which would have provided additional information regarding the vegetation cover, topography, or surface temperature. Despite these limitations, some agreement was found between the satellite and in-situ observations [Njoku *et al*, 2000]. A soil moisture retrieval method based on the microwave polarization difference index was also developed. This method used a nonlinear iterative optimization procedure with the horizontal and vertically polarized brightness temperatures at 6.6 Ghz and the vertically polarized brightness temperature at 37 GHz to simultaneously solve for vegetation depth and soil moisture. A soil roughness parameter was not included, as the authors found the effect of surface roughness to be small in areas that do not include mountainous terrain or extreme relief. Soil moisture was estimated over two study sites in Illinois for six years and compared to ground observations from three Illinois Water Survey Stations and found to coincide quite well despite differences in spatial resolution, vertical resolution, acquisition times, and observation periods. The greatest disparities between the two data sets occurred during the period of peak vegetation [Owe *et al*, 2001]. This work was later extended to include four test sites (Turkmenistan, Russia, Mongolia, and Iowa). Once again, no vegetation biophysical parameters were utilized for calibration purposes. The satellite measurements and in-situ observations were found to be generally in agreement [de Jeu, Owe, 2003]. These studies of soil moisture retrieval using SMMR provided a foundation for developing algorithms for AMSR-E and TMI. Owe and de Jeu have developed a new global surface soil moisture dataset which is consistent in its retrieval approach for its entire span, from November 1978 through the end of 2007. This dataset is derived using

all available historical and active satellite microwave sensors, including SMMR, SSM/I, TMI, and AMSR-E [Owe *et al*, 2008].

The Advanced Microwave Scanning Radiometer for EOS (AMSR-E) was launched in June 2002 and since that time has provided *the only* official NASA Level 3 soil moisture product. This product is retrieved using an algorithm developed by Dr. Eni Njoku of the Jet Propulsion Laboratory [Njoku, 1999]. The AMSR-E is a six-frequency, dual-polarized microwave radiometer that flies aboard Aqua at an orbital altitude of 705 km. The AMSR-E utilizes a 1.6 meter offset parabolic reflector with a constant incidence angle of approximately 55°. The dynamic range of measurement is 2.7-360 K. The sensor specifications of the AMSR-E are described in Table 3. The lowest frequencies of the AMSR (6.9 and 10.7 GHz) are sensitive to surface soil moisture under low vegetation cover conditions. These frequencies have better vegetation penetration at a cost of lower resolution. Although the algorithm originally utilized both the 6.9 and 10.7 GHz frequencies, the 6.9 GHz channel was found to be susceptible to Radio Frequency Interference (RFI). For this reason, the current version of the NSIDC soil moisture product uses only the 10.7 GHz channel [Njoku and Chan, 2005]. The estimated accuracy of the standard surface soil moisture product is 0.06 g/cm³ [Njoku, 1999].

Table 3- AMSR-E Sensor Specifications

Center Frequency (Ghz)	6.925	10.65	18.7	23.8	36.5	89.0
Bandwidth (MHz)	350	100	200	400	1000	3000
Mean Spatial Resolution (km)	56	38	21	24	12	5.4

Aqua has a sun-synchronous, near-polar orbit which results in valid grid cell counts which vary on a daily basis over a particular area, depending on latitude. The AMSR-E swath coverage pattern for descending passes as a function of latitude [Njoku, 2003]. In the case of Oklahoma, the latitude is about 35°. Any point at this latitude falls within the AMSR-E swath approximately every other day, with occasional daily sampling. Daily coverage is nearly 100% above and below 45° and complete coverage is achieved at 60° latitude.

Soil moisture over Iowa was retrieved by McCabe, Gao and Wood using the AMSR-E 10.7 GHz horizontally polarized brightness temperatures for June and July of 2002 and compared to SMEX02 ground measurements. This region was chosen due to its characteristic dense vegetation. Vegetation water content was estimated using monthly 1 km MODIS land cover classification and leaf area index data. Daily averages of ascending and descending measurements for 8 days were computed. A comparison with measurements from the Walnut Creek, Iowa SCAN station revealed a strong correlation between the data for the period of June 20 until July 4, 2003 although pixel-to-point scale and measurement disparities were noted. A comparison with areally averaged in-situ measurements from the SMEX02 experiment found that despite the inherent differences (physical estimation technique, scale, and sampling depth) between the measurements, there was a correlation of 0.75 with SMEX02. On a regional scale,

dominant trends were retained although local-scale responses were not [McCabe, Gao, Wood, 2005; McCabe, Wood, Gao, 2005].

Although the C-Band (6.9 GHz) is more sensitive to soil penetration it is also more vulnerable to RFI. Multiple swaths of AMSR-E data over the United States were analyzed and an RFI Index (RI) was computed which measures the difference between brightness temperature at 6.9 and 10.7 GHz at vertical and horizontal polarizations. This approach is based on the rationale that the dielectric properties of water in soils and vegetation lead to an increase in emissivity with frequency, so in the absence of RFI, the brightness temperature at 10.7 GHz is expected to exceed that at 6.9 GHz. The RFI index indicated that RFI was widespread, occurring mostly at or near major U.S. cities or airports. The locations of the RFI did not vary from day to day although the intensities were different for ascending and descending passes [Li *et al*, 2004].

This analysis was extended to the global land domain and for a one year observation period beginning with June 2002 and ending with May 2003 by the same authors, including Njoku and Li, in 2005. Six RFI indices were computed using the same spectral difference method applied to the 6.9, 10.7 GHz channels and the 10.7, 18.7 GHz channels at both vertical and horizontal polarizations and at multiple resolutions. The mean and standard deviations of this index for July 2002 and January 2003 were computed and binned on a 0.25° grid. Lower prevalence of RFI was found at 10.7 GHz than at 6.9 GHz. The authors found that strong and persistent RFI at 6.9 or 10.7 GHz may be identified by large magnitudes of both means and standard deviations of the corresponding RFI indices at vertical polarization. The vertically polarized indices

provided better RFI discrimination due to the greater influence of geophysical variability on the horizontally polarized brightness temperatures. Fixed or time-varying thresholds may be used to generate masks for rejecting RFI contaminated AMSR-E data [Njoku *et al*, 2005].

The TRMM TMI may also be used to estimate soil moisture, although no official NASA soil moisture product is available for this instrument. TRMM was launched in 1998 and has continued to provide useful data for over 10 years. TMI is based on the SSM/I design, with an additional dual-polarized 10.65 GHz (X-Band) channel that is useful for soil moisture retrieval. TMI utilizes an offset parabolic antenna and a constant incidence angle of approximately 52.8° at the surface. TRMM utilizes an orbital altitude of 350 km, which allows successive scans to overlap (except in the 85.5 GHz channel, which has the smallest footprint). However, as its name implies, TRMM was designed to focus on the tropical regions, thus its main limitation is its spatial coverage. TRMM's near-equatorial orbit is less straightforward than the polar orbits utilized by the other satellites in that local overpass times vary throughout the 24 hour day, making a complete cycle approximately every month. This variation in sampling time complicates comparisons with ground measurements.

Microwave sensors such as SMMR, AMSR-E, and TMI have shown some success in retrieving soil moisture over certain areas but have also been hampered by their low spatial resolutions of about 50 km. Optical/IR sensors such as MODIS provide much better spatial resolution (~ 1 km) but are sensitive to soil type as well as moisture [Chauhan *et al*, 2003].

The National Polar-orbiting Operational Environmental Satellite System (NPOESS) will unify existing polar orbiting satellites under a single national program. The launch of the first operational NPOESS spacecraft is currently planned for 2013 [Griffin, 2006]. It will be a joint effort which will be managed by the Integrated Program Office, drawing on existing expertise from the Department of Commerce, the Department of Defense and the National Aeronautics and Space Administration. Originally, plans for the NPOESS instruments included the Visible/Infrared Imager Radiometer Suite (VIIRS) and the Conical-Scanning Microwave Imager/Sounder (CMIS).

VIIRS will collect visible and infrared imagery and radiometric data using 22 bands. It is based on the AVHRR and the MODIS. Planned VIIRS Environmental data records (EDRs) include NDVI, SST, ocean color, and cloud properties [Puschell *et al*, 2003]. The CMIS would have been a six-band radiometer with capabilities similar to AMSR-E. However, the CMIS sensor was discontinued in June 2006 by the Nunn-McCurdy certification decision and replaced with the simpler, cheaper Microwave Imager/Sounder (MIS). The MIS will not be ready for the C1 (2013) Mission and so will only be flown on C2 (2016), C3 (2018), and C4 (2020), resulting in a discontinuity of AMSR-E products [NASA/NOAA, 2007].

An improved resolution soil moisture product can be obtained using a synergistic optical/IR and microwave approach. First, a passive microwave radiometer is used to measure brightness temperature, which is then inverted using a radiative transfer model similar to that used by AMSR-E to obtain low resolution (50 km) soil moisture. Second, a regression analysis is applied to VIIRS optical/IR measurements (NDVI, albedo, and

LST) and the low-resolution soil moisture to obtain high resolution (1 km) soil moisture. NDVI is used to determine the vegetation present in the area. The retrieval algorithm is limited to $NDVI \leq 0.4$ (weakly vegetated areas such as grassland and short agricultural crops).

The VIIRS soil moisture algorithm theoretical basis document (ATBD), written by Zhan and others in 2002, describes two possible techniques for retrieval. If the Microwave Imager/Sounder (MIS) has two polarizations, the ratio of brightness temperatures at horizontal and vertical polarizations can be used to obtain horizontal (R^h) and vertical (R^v) Fresnel reflection coefficients. The dielectric constant can be expressed in terms of these reflectivities and then converted to obtain soil moisture. If only a single polarization is available, the authors propose assuming that the single-scattering albedo is negligibly small, in which case brightness temperature is a function of vegetation optical depth, τ_c , and emissivity, e_s . Emissivity can be expressed as a function of the Normalized Difference Vegetation Index (NDVI). Either of these techniques can be used to obtain low-resolution soil moisture [Zhan *et al*, 2002].

A relationship between surface soil moisture, surface radiant temperature, and fractional vegetation has been demonstrated and can be described by the “universal triangle” [Carlson *et al*, 1994]. Brightness temperature and NDVI are scaled (T^* , $NDVI^*$) with respect to their minimum and maximum values. Soil moisture is lowest when brightness temperature is high or NDVI is high and highest when both brightness temperature and NDVI are low. Soil moisture (M) can therefore be approximated with a second-order polynomial fit:

$$M = a_{00} + a_{10}NDVI^* + a_{20}NDVI^{*2} + a_{01}T^* + a_{02}T^{*2} \\ + a_{11}NDVI^*T^* + a_{11}NDVI^{*2}T^{*2} + a_{12}NDVI^*T^{*2} + a_{21}NDVI^{*2}T^*$$

Land surface temperature (LST) and NDVI are official planned VIIRS Environmental Data Records (EDRs), as is surface albedo. The LST, NDVI, and surface albedo products are available at high-resolution but are aggregated to the same resolution as the microwave radiometer product. As described above, a regression analysis can be used to obtain coefficients relating soil moisture to LST, NDVI, and surface albedo. This relationship can then be used to obtain high resolution soil moisture from the original (1 km) LST, NDVI, and surface albedo products. A unique relationship between these parameters may exist for any particular region. Results are best when the training area (where the regression coefficients are determined) is the same as the test area (where the relationship is applied) [Gillies *et al*, 1997]. An integrated system of soil moisture retrieval using AMSR-E and MODIS measurements was developed and utilized by EastFIRE Laboratory at George Mason University [Hao *et al*, 2006].

The authors of the VIIRS Soil Moisture ATBD applied their algorithm to data from the Southern Great Plains field campaign in June and July of 1997 (SGP-97). SGP-97 included in-situ point measurements made at three sites: Little Washita (LW), El Reno (ER), and Central facility (CF). SSM/I-derived 25-km soil moisture, and aggregated AVHRR LST, NDVI, and surface albedo were used to form a regression relationship, which was then used to estimate 1-km soil moisture. A consistent and definite pattern of daily spatial variability was observed at all three sites over the four days. Low resolution and high resolution soil moisture were compared to each other and to ground data

obtained in the field campaign and a consistent decreasing trend was observed in all data for June 29-30 and July 1-2.

The “universal triangle” relationship was subsequently applied to an area in eastern China by L. Wang and others in 2007. Ground measurements made at a depth of 10 cm were obtained from a network of 137 stations. NDVI and LST were obtained at 1 km resolution from MODIS over the same area. Two years (2003-2004) of data were obtained and used for calibration and one year (2005) was used for validation. Correlation coefficients were obtained and found to be greater than 0.5 at 90 stations and greater than 0.8 at 55 stations. These results demonstrate a correspondence between the satellite and ground data, despite the differences in sampling depth. The algorithm performed satisfactorily in cropland and grassland, which accounted for 85% of the study area [*Wang et al*, 2007].

In addition to the NPOESS, other future missions which plan to provide a standard soil moisture product include the Soil Moisture and Ocean Salinity Mission (SMOS) and the Soil Moisture Active-Passive (SMAP) Mission. The Soil Moisture and Ocean Salinity (SMOS) Mission is scheduled for launch in 2009 by the European Space Agency. A major science objective of the mission is surface soil moisture with an accuracy of $0.04 \text{ m}^3/\text{m}^3$ and a revisit time of 2-4 days. SMOS utilizes basic interferometric principles to obtain passive microwave data at 1.4 GHz (L-Band) [*SMOS Mission Objectives and Scientific Requirements*, 2002]. This is accomplished by the Microwave Imaging Radiometer using Aperture Synthesis (MIRAS), which is based on the design of NASA’s Electronically Scanned Thinned Array Radiometer (ESTAR).

ESTAR proved its usefulness in several USDA field campaigns. The MISAR utilizes an antenna array with 133 elements, each of which is connected to a Monolithic Microwave Integrated Circuit L-band receiver. The received signals are amplified, down-converted, digitized, and correlated to obtain a visibility function which can be inverse Fourier transformed into the brightness temperature. Dual polarizations (horizontal and vertical) are used. The use of a synthetic aperture radiometer was motivated by the increased sensitivity of L-band to soil moisture content due to the decreased effects of vegetation attenuation and surface roughness at these frequencies (*Martin-Neira, 1997*).

The Soil Moisture Active-Passive (SMAP) Mission is a future NASA mission planned for launch in 2012. It is based on the development made for the Hydros Mission, which was cancelled in 2005 due to budget limitations. The SMAP is currently in Phase A and addressing numerous issues related to the L3 soil moisture retrieval algorithms. A new strategy for soil moisture measurement planned for use in Soil Moisture Active Passive Mission is the use of concurrent active-passive remote sensing [*Soil Moisture Active Passive Validation Experiment 2008 Experiment Plan, 2008*].

The SMAP orbit is planned to be sun-synchronous, with an altitude of 670 km. A global revisit time of about 3 days is desired. The main goal of SMAP is to obtain global observations of soil moisture and the freeze/thaw state. SMAP will include synthetic aperture radar (1.26 GHz) and a radiometer (1.41 GHz). The radar will have a resolution of 10 km while the radiometer will have a resolution of 40 km. Both instruments will utilize dual-polarization. The scientific measurement requirements for soil moisture are $\sim\pm 0.04 \text{ m}^3/\text{m}^3$ volumetric accuracy in the top 2-5 cm of soil, for vegetation water content

$< 5 \text{ kg/m}^2$. SMAP soil moisture algorithm development currently includes three possible streams: (1) passive only at 40 km resolution, (2) active only at 1-3 km resolution, and (3) combined active/passive at 10 km resolution. The high accuracy of passive techniques and high resolution of active retrieval may be combined to obtain an improved product [SMAP Mission NASA Workshop Report, 2007].

The main challenge is the large size of the antenna (~6 meter aperture) needed for L-band. Deployable mesh reflector technology will make this possible. In addition, the SMAP antenna will need to be capable of rotating at a rate of 14.6 rpm to maintain the minimum overlap needed between tracks. Both the radar and the radiometer will benefit significantly from the RF electronics developed for the Aquarius Mission. A digital radiometer back-end will allow for on-board implementation of RFI mitigation algorithms. Possible demonstrated techniques include:

1. time domain (detection of spikes in the data)
2. frequency domain (bandwidth subdivision to identify channels with anomalous brightness)
3. kurtosis (use of the fourth standardized moment as a measure of the probability distribution of the received fields)

Several possible RFI mitigations techniques exist. More data regarding RFI at L-band will be available from SMOS, and these results will be incorporated to determine the best approach for SMAP [SMAP Mission NASA Workshop Report, 2007].

THEORY

A gray body emits radiant power which is a function of its surface temperature T and its emissivity ϵ . The emissivity is a function of the properties of the surface, such as its composition and roughness. The surface temperature of the Earth is about 300 K and in any particular location will not vary by more than 60 K, a relative variation of about 20%. Differences in surface composition and roughness will cause much greater variations. For example, the variations in surface microwave temperature of three materials when observed from nadir at microwave frequencies are shown in Table 4 [Elachi and van Zyl, 2006]. A thermodynamic temperature (T_g) of 300 K and a sky temperature (T_s) of 40 K are assumed. The equivalent surface microwave temperature of sand is double that of water.

Table 4- Microwave Temperature of Three Representative Types of Material

Type of Material	Index of refraction, n	Dielectric constant	Normal reflectivity	Microwave Temperature (K)
Water	9	81	.64	134
Solid rock	3	9	.25	235
Sand	1.8	3.2	.08	280

The basis of soil moisture retrieval algorithms is the large difference in the dielectric properties of dry soil (~ 4) and water (~ 80). The dielectric constant of a substance is the ratio of the permittivity of the substance to the permittivity of free space.

In the case of a water molecule, the negative charge is concentrated at the oxygen atom and the positive charge is concentrated at the hydrogen atoms, forming an electric dipole. When an electromagnetic field is applied to water, the molecules align in response, resulting in a large dielectric constant. The dielectric constant of soil increases as water content increases, which has a measurable effect on the microwave emission from soil. The variation of the surface dielectric constant as a function of soil moisture has been measured by several researchers for different types of soil. One example of variations in L-Band (1.4 GHz) brightness temperatures due to soil moisture is shown in Figure 2. These results are from the Monitoring Underground Soil Experiment (MOUSE) field campaign which took place in Northern Italy in 2004 [Vall-Ilossera et al, 2005]. It is clear that the variation due to soil moisture is significant. The surface temperature decreases by more than 70 K as the soil moisture increases from dry to saturated.

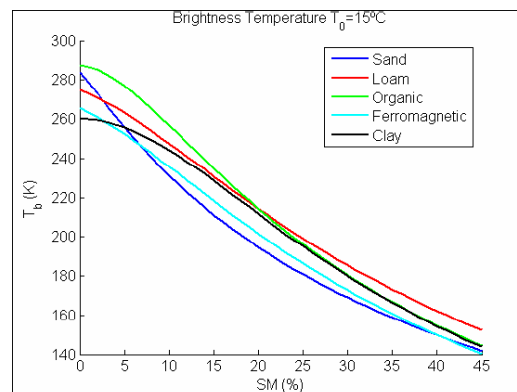


Figure 2- Variations in dielectric constant as a function of soil moisture (Source: Vall-Ilossera et al, 2005)

The presence of vegetation complicates the measurement of soil moisture, because vegetation absorbs or scatters the radiation emitted by the soil and also emits its own radiation. The attenuation of vegetation is characterized by the vegetation optical

depth, τ_c and is directly related to vegetation water content, W_c , by the relationship $\tau_c = bW_c$ where b is the vegetation opacity coefficient that is determined experimentally. The trends in the relationship between b and wavelength indicate that vegetation can be divided into three categories: leaf-dominated (soybeans, cotton, alfalfa), stem-dominated (corn and wheat), and grasses. Excluding the grass observations, at L-band there is a small variation in b for all vegetation types. At these wavelengths, a single value of b may be used without significant error. A value of $b=0.15$ is representative of most agricultural crops [Jackson and Schmugge, 1991]. As vegetation cover increases, attenuation (and thus soil moisture retrieval error) increases, and for dense vegetation (with $W_c > 5 \text{ kg/m}^2$) no measurement at all is possible. Low frequencies between 1 and 3 GHz are best for soil moisture sensing because vegetation attenuation is less at longer wavelengths. However, the costs associated with supporting a large low-frequency antenna are prohibitive. As a result, remote sensing of soil moisture has primarily utilized microwave frequencies in the 6-10 GHz range.

The brightness temperature observed at the top of the atmosphere at a given incidence angle and frequency can be expressed by the radiative transfer equation. The equation of radiative transfer states that as a beam of radiation travels, it loses energy to the atmosphere by absorption, gains energy by emission, and redistributes energy by scattering. The AMSR-E Land Surface Parameters ATBD develops a model utilizing an absorbing vegetation layer above soil, as shown in Figure 3. All terms are defined in Table 5. It is worth noting that emissivity is a function of incidence angle.

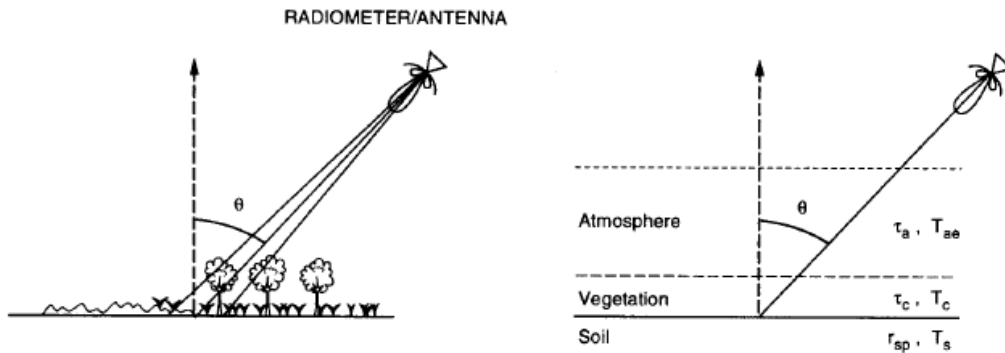


Figure 3- Model Representation of a Spaceborne Radiometer Viewing a Heterogeneous Earth Surface (Source: AMSR Land Parameters ATBD)

Table 5- AMSR-E ATBD Model Terms and Definitions

Term	Definition
T_{ae}	Temperature of the atmosphere
τ_a	Atmospheric optical depth
T_c	Vegetation temperature
τ_c	Vegetation optical depth
r_{sp}	Soil reflectivity
T_s	Effective soil temperature
ω	Vegetation single scattering albedo

The brightness temperature observed at the top of the atmosphere is the sum of the upwards contribution of the atmosphere, the downwards contribution of the atmosphere reflected by the soil and attenuated by the vegetation and atmosphere, the upwards contribution of the vegetation attenuated by the atmosphere, the downwards contribution of the vegetation reflected by the soil and attenuated by the atmosphere, and the contribution of the soil attenuated by the vegetation and atmosphere. An assumption is made that there is no reflection at the atmosphere-vegetation boundary. Multiple scattering in the vegetation layer is also neglected for the sake of simplicity. Let T_u

describe the upwelling atmospheric emission and T_d describe the downwelling atmospheric and space-background emission at the top of the vegetation. Each contributing factor to the radiative transfer equation is described in Table 6.

Table 6- Radiative Transfer Equation Contributing Factors
(Source: AMSR-E Land Parameters ATBD)

Description of Contribution	Equation
Upwards contribution of atmosphere	T_u
Downwards contribution of atmosphere, reflected by the soil and attenuated by the vegetation and atmosphere	$T_d \exp(-\tau_c) r \exp(-\tau_c) \exp(-\tau_a)$
Upwards contribution of vegetation, attenuated by atmosphere	$T_c (1-\omega)(1- \exp(-\tau_c)) \exp(-\tau_a)$
Downwards contribution of vegetation, reflected by the soil and attenuated by the vegetation and atmosphere	$T_c (1-\omega)(1- \exp(-\tau_c)) r \exp(-\tau_c) \exp(-\tau_a)$
Contribution of soil attenuated by the vegetation and atmosphere	$T_s e_s \exp(-\tau_c) \exp(-\tau_a)$

The relationship between the soil dielectric constant and the soil volumetric moisture is influenced by soil texture and surface roughness. For this reason, ancillary data describing soil texture and topography is critical in improving the accuracy of retrievals. Surface roughness and vegetation scattering effects become increasingly complex at frequencies greater than 10 GHz so the model is restricted to frequencies below this.

STUDY AREAS

The current study is conducted over one primary and one secondary area, both located in the Southern United States. AMSR-E, TMI, and MODIS soil moisture data over the Little Washita River Experimental Watershed and AMSR-E and TMI soil moisture data over the Little River Experimental Watershed were analyzed. These regions were chosen due to their locations within the spatial coverage of TMI, as well as due to the availability of free in-situ observations at these sites. Little Washita and Little River are experimental watersheds studied by the United States Department of Agriculture (USDA) Agricultural Research Service (ARS) [*Weltz and Bucks, 2003*]. Both areas contain stations which are part of the national Soil Climate Analysis Network (SCAN) maintained by the USDA Natural Resources Conservation Service. The Little Washita and Little River Experimental Watersheds were also chosen as areas of study by Jackson in AMSR-E validation activities [*Jackson et al, 2006*].

The Little Washita River Experimental Watershed (LWREW) covers parts of Comanche, Caddo, and Grady counties and is shown below in Figure 4. The closest major city is El Reno, Oklahoma. The area is composed of 611 square kilometers in the southwest part of Oklahoma. The LWREW has a semi-humid climate with a mean annual temperature of 16°C and annual rainfall of 760 mm. Most of the precipitation occurs in the spring and fall. The distribution of precipitation in Oklahoma generally has

two peaks during the year. The largest peak is in late spring, and the secondary peak is in early fall. June and October are usually the wettest months. Most precipitation falls during the night although the maximum rainfall intensity typically occurs in the late afternoon. Much of the precipitation comes in the form of short intense storms which cause excessive runoff. Precipitation variability is an important issue in the agriculturally intensive areas which are particularly vulnerable to droughts and floods. The soil type ranges from fine sand to silty loam [Elliott *et al*, 1993].

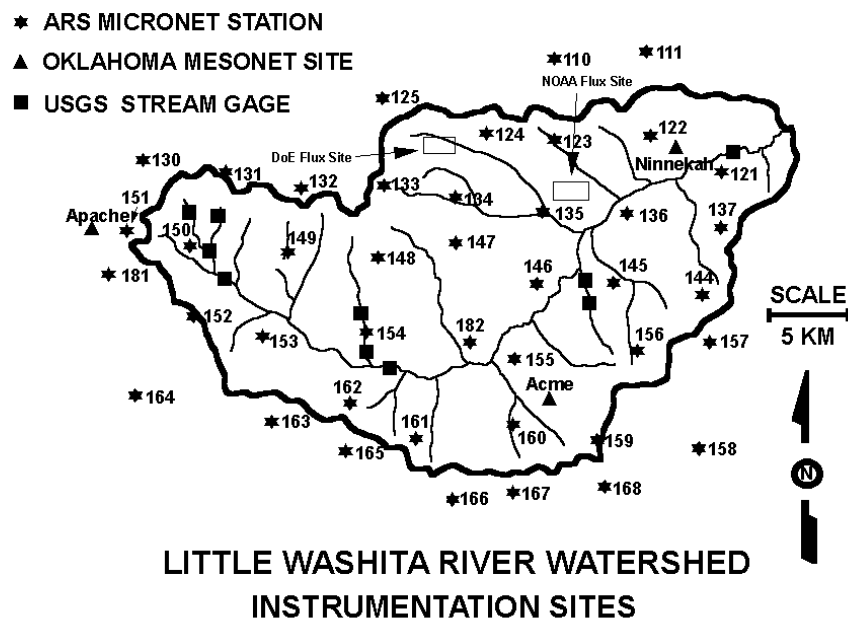


Figure 4- Little Washita River Experimental Watershed
 (Source: USDA ARS Micronet Data for SGP97, 1999)

Surface cover in the LWREW is dominated by pasture, rangeland and winter wheat and also includes crops such as corn and alfalfa. Winter wheat is harvested in June and July. Corn is harvested in August, September, and October. Alfalfa is harvested

April through December [*Oklahoma Ag in the Classroom*, 2008]. Therefore, the LWREW year can be divided into a non-crop-covered November through April period and a crop-covered May through October period. January, February, and March were chosen as representative months for the non-crop-covered period and June, July, and August were chosen as representative months for the crop-covered period.

The LWREW is a particularly good study area because it has been the subject of extensive hydrologic research by the USDA ARS since 1961 [*Allen*, 1991]. The joint NASA-NOAA-USDA Soil Moisture Experiment (SMEX) in 2003 included this area. The ARS currently monitors the LWREW with a 20-station network called the OKMESO Little Washita Micronet which measures rainfall, relative humidity, air temperature, solar radiation, soil temperature, and volumetric water content. The LWREW also includes two stations from the Oklahoma Mesonet (Acme and Apache) which measure soil moisture. In addition, the one of the USDA SCAN stations is located within the LWREW.

The Little River Experimental Watershed (LREW) is located in southern Georgia. It is one of the USDA Agricultural Research Service's experimental watersheds. This area has a humid climate, with mean annual rainfall of 1200 mm. The topography is flat. 50% of the region is woodland, 31% is row crops (primarily peanuts and cotton), 10% is pasture, and 2% is water [*Jackson et al*, 2006]. Tifton, Georgia, the closest city to LREW, had a median growing season of 259 days from 1961 until 1990 (as defined by temperatures above 32° C). The last spring frost occurs around March 6 and the first fall frost occurs around November 21 [*Southeast Regional Climate Center*, 1997].

DATA SOURCES

SCAN Data

In-situ soil moisture measurements from the SCAN are available from the National Water and Climate Center. The advantage of the SCAN is its ability to provide long-term continuous, real-time data. SCAN station 2023 is located within the LWREW, at 34°57'N 97°59'W. SCAN station 2027 is located within the LREW, at 31.5° N, 83.55° W.

Each SCAN station includes several Stevens-Vitel Hydra Probe sensors which use an electromagnetic signal propagated from the probe to measure the electrical properties of the soil, including soil moisture. The technical specifications of the Hydra Probe are provided in Table 7 [*Stevens Water Monitoring Systems, Inc*]. These sensors provide hourly soil moisture percentage at depths of 2, 4, 8, 20, and 40 inches. The AMSR-E at 10.7 GHz approximates the measurement of 0.5 cm near-surface soil moisture, so the sensor located at the shallowest depth (C1SMV) is most appropriate for comparison.

At the Little Washita study site, SCAN station 2023 has been in operation from November 10, 1998 until present. However, the SCAN site has the largest mean relative difference from the watershed average and the largest standard deviation of all the LWREW soil moisture sensors. The SCAN site reports higher soil moisture values than the other ground observation stations. The SCAN station also exhibits less temporal

stability than the Micronet. This may be due to the site's position along a ridgeline [Cosh *et al*, 2006]. For this reason, the SCAN station data was not used as a source of in-situ measurements for the LWREW.

**Table 7- Technical Specifications of Stevens-Vitel Hydra Probe
(Source: Stevens Water Monitoring Systems, Inc)**

Measurements	Range	Accuracy
Dielectric constant	1 to 78 where 1 = air, 78 = distilled water	± 1.5% or 0.2 whichever is typically greater
Soil Moisture	From completely dry to fully saturated	± 0.03 water fraction by volume in typical soil
Conductivity	0.01 to 1.5 S/m	± 2.0% or 0.005 S/m whichever is typically greater
Temperature	-10° to +65° C	± 0.1° C

Oklahoma Mesonet Data

The Oklahoma Mesonet is an automated network of 116 meteorological stations throughout the state of Oklahoma operated by the Oklahoma Climatological Survey. There is at least one station located in each of Oklahoma's 77 counties. No other state contains such a complete network of environmental monitoring stations. Each station measures air temperature, relative humidity, wind speed and direction, barometric pressure, rainfall, incoming solar radiation, and soil temperatures. In 1996, the Mesonet installed Campbell Scientific 229-L heat dissipation sensors in 60 sites. Soil moisture temperature is measured every 30 minutes at depths of 5, 25, 60, and 75 cm (when possible). An initial temperature is measured, a heat pulse is introduced using a 50-mA current, and a final temperature is measured. The calibrated change in temperature of the soil (ΔT_{sensor}) is the official variable reported by the Mesonet.

Soil matric potential, the capillary force needed to retain water in the soil, may be obtained from the calibrated temperature of the soil equation 1 below [Illston et al, 2008].

The calibration constants were obtained through laboratory tests by Mesonet scientists.

$$MP = -c \cdot \exp(a \cdot \Delta T_{ref}) \quad (WT = -MP) \quad (1)$$

where

- MP = soil matric potential (kPa)
- WT = soil water tension (kPa)
- a = calibration constant (1.788 °C⁻¹)
- c = calibration constant (0.717 kPa)
- ΔT_{ref} = reference temperature differential (°C)

In turn, volumetric water content may be derived from soil matric potential using equation 2 below [Illston et al, 2008]. Empirical coefficients (a and n) and soil characteristics (WC_r and WC_s) are site-specific and may be obtained at

<http://mesonet.org/sites/geomeso.csv>.

$$WC = WC_r + \frac{WC_s - WC_r}{\left(1 + \left(a \cdot \frac{-MP}{100}\right)^n\right)^{\left(\frac{1}{n}\right)}} \quad (2)$$

where

- WC = soil water content on a volume basis (m³_{water} / m³_{soil})
- WC_r = residual water content (m³_{water} / m³_{soil})
- WC_s = saturated water content (m³_{water} / m³_{soil})
- α = empirical constant (kPa⁻¹)
- n = empirical constant (unitless)
- MP = matric (soil-water) potential (kPa)

Mesonet stations Acme and Apache are contained within the LWREW and both stations include soil moisture sensors. Acme, station 110, is located at 34.808330° N, 98.023250° W in Grady County. At 5 cm of depth, the soil is sandy loam, 73.43% sand, 17.69% silt, and 8.88% clay. Apache, station 111, is located at 34.914180° N,

98.292160° W. At 5 cm of depth, the soil is sandy loam, 84.33% sand, 10.62% silt, and 5.04% clay. Among the variables reported in the Mesonet public data files are TR05, TR25, TR60, and TR75, the calibrated differences between the final and starting soil temperatures at 5, 25, 60, and 75 cm respectively. TR05 is most practical for use in validating skin soil moisture obtained from passive microwave remote sensing.

However, since soil volumetric water content is not calculated explicitly and the data is not available for free to the public, the Oklahoma Mesonet was not used as a source of in-situ measurements in this study.

Agricultural Research Service Micronet Data

The U.S.D.A. Agricultural Research Service (ARS) operates an automated network of 42 stations called the ARS Micronet. This small high-density network is part of the larger Oklahoma Mesonet. Each Micronet station measures total rainfall, total solar radiation, relative humidity, air temperature, and soil temperature. In addition, as part of the AMSR-E Validation Program, Hydra Probe soil moisture sensors were installed in 11 ARS Micronet sites in 2002. Soil temperature is measured at 5, 10, 15, and 30 cm below the ground surface. Volumetric soil water content (VW) is measured by a Stevens-Vitel Hydra Probe (Stevens Water Monitoring Systems, Inc.) every 30 minutes at depths of 5, 25, and 45 cm. The standard unit of the measurement is fractional percentage. The sensor has an accuracy of ± 0.03 water fraction by volume in typical soil. The latitude and longitude coordinates and soil type of each of the ARS Micronet stations are listed in Table 8, as well as the temporal range of the data. The algorithms to

calculate soil parameters from the Hydra Probe sensors require a soil type. Three soil types are currently used: sand, silt, or clay.

Table 8- ARS Micronet Station Information (Source: ars.mesonet.org)

Station ID	Latitude	Longitude	Soil type	Temporal Range
Berg	35.0453 N	97.9167 W	silt loam	2002 – August 2004
111	35.0159 N	97.9518 W	silt	2002 - January 2005
133	34.9491 N	98.1281 W	sand	2002 - Present
134	34.9366 N	98.0753 W	sand	2002 - Present
136	34.9277 N	97.9656 W	silt	2002 - Present
144	34.879 N	97.9171 W	sand	2002 - Present
146	34.8854 N	98.0231 W	silt	2002 - Present
149	34.8984 N	98.1809 W	silt	2002 - Present
151	34.9133 N	98.2928 W	sand	2002 - February 2005
154	34.8552 N	98.137 W	silt	2002 - Present
159	34.7966 N	97.9932 W	sand	2002 - Present
162	34.8133 N	98.1417 W	sand	2002 - Present

The soil moisture measurements from the ARS Micronet sites were used as a primary source of in-situ data. The ARS Micronet is operated and maintained by Grazinglands Research Laboratory in cooperation with Oklahoma State University and the Oklahoma Climatological Survey. Monthly Ascii files containing average, maximum, and minimum daily values are available for each station. Each daily value is accompanied by a data quality control flag that describes the results of quality tests on the data.

The temporal stability of LWERW Micronet soil moisture measurements were analyzed by the USDA ARS, including Michael Cosh and Tom Jackson. 30 minute 5-cm depth data from 13 stations (including Berg and NOAA) from July 2002 to April 2004 was used. A watershed average was computed by Cosh and Jackson using all of the

Micronet stations data. Measurements from SCAN station 2023 were also obtained and compared to the Micronet measurements. The standard deviations were found to be less than 30% for all stations except the NOAA Micronet station and the SCAN station. Micronet stations 146, 149, 162, and Berg demonstrated the smallest mean relative difference values and standard deviations compared to the watershed average. This indicates that these four sites are most representative of the area. These four sites exhibit a variety of soils, from silt to sand. They are not centrally located in the watershed, as shown in Figure 4. They appear to share no distinctive quality that would indicate temporal stability. The NOAA Micronet station is located about 50 meters north of the SCAN site and utilizes the same Vitel sensor to measure soil water content. Higher soil moisture values than average were also measured at the NOAA station [*Cosh et al, 2006*]. Data from the Berg site was used in this study.

AMSR-E Data

Daily gridded AMSR-E Level 3 soil moisture data were obtained in HDF-EOS format from the National Snow and Ice Data Center (NSIDC). Each file contains both ascending and descending pass measurements. Over the United States, Aqua's ascending pass is during the daytime and its descending pass is during the nighttime. In this study, only nighttime (descending pass) data were used because of the greater stability of nighttime surface temperatures [*Owe et al, 2001*]. AMSR-E provides global land surface coverage ($\pm 86.72^\circ$). It was launched aboard Aqua in June 2002 and since that time has provided the *only* official NASA Level 3 soil moisture product. The algorithm used for retrieving this product was developed by Eni G. Njoku of the Jet Propulsion Laboratory.

Aqua utilizes a sun-synchronous, near-polar orbit with a 1:30 AM descending node and a 1:30 PM ascending node. Therefore, Aqua travels north across the equator at 1:30 PM local time (ascending, daytime pass) and south across the equator at 1:30 AM local time (descending, nighttime pass). As LWREW is located north of the equator, the satellite's nighttime observation over this area occurs before 1:30 AM.

The AMSR-E Soil Moisture data utilizes the Equal-Area Scalable Earth (EASE) full global (ML) Grid, with a spatial resolution of approximately 25 km. As the name suggests, this grid is equal area, so all cells have the same area. The slightly larger exact cell size of 25.067525 km allows the grid to exactly span the equator. The EASE ML grid is defined by 1383 columns (x) and 586 rows (y) and so that the point where the equator crosses the prime-meridian occurs at cell location (691.0, 292.5). Grid coordinates (x,y) begin at the upper left corner at cell (0,0), with x increasing to the right and y increasing downwards. The grid utilizes $\pm 30^\circ$ for its standard parallels, which minimizes the angular distortion over the continents and makes this projection particularly useful for studying mid-latitude regions such as Oklahoma [Brodzik and Knowles, 2002]. The file contains fill data values of 9999 and -9999. A fill value of 9999 indicates a pixel that is void of retrieval due to inherent gaps between available L2A swaths. A fill value of -9999 indicates a pixel that is void of retrieval due to bad temperature data or screening by land surface classification or retrieval values outside the physical range. Valid soil moisture values are expected to be between 0 and 500, and when scaled to standard scientific units range from 0 to 0.5 g/cm³ range [Njoku, 2004].

In the case of the Little Washita River Experimental Watershed (Oklahoma), a single $0.25^\circ \times 0.25^\circ$ grid cell of AMSR-E data containing the Berg Micronet station was obtained, with a bounding box of $98^\circ \text{ W} - 97.75^\circ \text{ W}$, $35^\circ \text{ N} - 35.25^\circ \text{ N}$. In the case of the Little River Experimental Watershed (Georgia), a single $0.25^\circ \times 0.25^\circ$ grid cell of AMSR-E data containing the SCAN site was obtained with a bounding box of $83.75^\circ \text{ W} - 83.5^\circ \text{ W}$, $31.5^\circ \text{ N} - 31.75^\circ \text{ N}$.

TRMM Data

Daily gridded Level 2 TMI soil moisture data was obtained in HDF format from Princeton's Land Surface Hydrology Research Group. Each file contains daily-averaged (using both ascending and descending passes) quality-screened measurements. The spatial resolution is $1/8^\circ$. The format of the file is binary (little-endian). Each grid cell is represented by a 4-byte integer. Each file contains 464 columns representing longitudes from 125° W to 67° W (a range of 58° , with one grid cell per $1/8^\circ = 464$ grid cells) and 112 rows representing latitudes from 25° N to 39° N (a range of 14° , with one grid cell per $1/8^\circ = 112$ grid cells). As TRMM was designed to focus on the tropical regions, the main limitation of this satellite's data is its spatial coverage, which is $\pm 38^\circ$.

Daily soil moisture retrievals using the Princeton algorithm are available from 1998 through 2004. The standard unit of the measurement is fractional percentage. Several masks are used for quality control. A precipitation mask uses hourly precipitation data from the NLDAS system to remove retrievals for grid boxes with falling precipitation. A vegetation sensitivity mask utilizes monthly averaged polarization ratios to remove low variability areas which were suspected to contain heavy

vegetation. A snow cover, frozen soil, and surface water contamination mask uses daily frozen soil and snow classification data from the NSIDC to mask areas where the algorithm for calculating the soil dielectric constant was no longer applicable. Areas that are masked out have a value of 0. Areas where there are no TMI retrievals have a fill value of 9.999×10^{20} . All retrieved soil moisture values are greater than zero [*Gao et al*, 2006].

In the case of the Little Washita River Experimental Watershed (Oklahoma), a single $0.125^\circ \times 0.125^\circ$ grid cell of TMI data containing the Berg Micronet site was obtained with a bounding box of $98^\circ \text{ W} - 97.875^\circ \text{ W}$, $35^\circ \text{ N} - 35.125^\circ \text{ N}$. In the case of the Little River Experimental Watershed (Georgia), a single $1/8^\circ \times 1/8^\circ$ grid cell of TMI data containing the SCAN site was obtained with a bounding box of $83.675^\circ \text{ W} - 83.5^\circ \text{ W}$, $31.5^\circ \text{ N} - 31.675^\circ \text{ N}$. Note that the TMI snow and frozen soil mask was used in January and February of 2003, resulting in 13 valid days of TMI soil moisture data in January and 14 valid days in February.

The Daily TRMM and Other Rainfall Estimate (3B42 V6 derived) data were also obtained by the author. This data includes daily accumulated rainfall in millimeters at a resolution of $1/8^\circ \times 1/8^\circ$. The data were obtained using the TRMM Online Visual and Analysis System (TOVAS), <http://lake.nascom.nasa.gov/tovas/>. This system was developed and is supported by the GES DISC. TOVAS is a member of the Giovanni (GES-DISC On-line Visualization and Analysis System) family.

MODIS Data

MODIS Aqua Level 1 data were obtained from the Goddard Space Flight Center (GSFC) Level 1 and Atmosphere Archive and Distribution System

(<http://ladsweb.nascom.nasa.gov/data/>). Only daytime granules are relevant because MODIS utilizes optical and infrared frequencies. These products are listed in .

MYD11_L2 was obtained from NASA's Warehouse Inventory Search Tool (WIST), <http://wist.echo.nasa.gov>.

Table 9- MODIS Product Names and Descriptions

MODIS Product Name	Description
MYD021KM	MODIS Aqua Level 1B Calibrated Radiances- 1 km
MYD02QKM	MODIS Aqua Level 1B Calibrated Radiances- 500 m
MYD02HKM	MODIS Aqua Level 1B Calibrated Radiances- 250 m
MYD03	MODIS Aqua Level 1B Geolocation
MYD11_L2	MODIS Aqua Level 2 Land Surface Temperature

Field Campaigns

Evaluating satellite soil moisture products is extremely difficult due to a lack of dense ground networks. The AMSR-E validation plan included several soil moisture field campaigns (SMEX02, SMEX03, SMEX05) which were intended to gather detailed soil moisture data. Major Field campaigns which took place within the United States and utilized airborne microwave instruments are shown in Table 10. The USDA Agricultural Research Service (ARS) is intensely involved in these campaigns, usually coordinated by Dr. Thomas Jackson of the USDA-ARS Hydrology and Remote Sensing Lab.

Table 10- Major U.S. field campaigns using airborne microwave instruments
 (Source: *USDA ARS Soil Moisture Experiments: Washita, SGP, SMEX, and CLASIC, 2008*)

Field campaign	Location	Time period
Washita '92	Oklahoma	June 1992
Washita '94	Oklahoma	April 1994
Southern Great Plains '97	Oklahoma	July 1997
Southern Great Plains '99	Oklahoma	July 1999
SMEX02	Iowa	June 24-July 15, 2002
SMEX03	Oklahoma, Georgia, Alabama	June 23-July 18, 2003
SMEX05	Iowa	June 2005
CLASIC	Oklahoma	June 2007

METHODOLOGY

Ground soil moisture measurements at a depth of 5 cm were obtained by the author from the Berg ARS Micronet station for 2003. These measurements are available at 30 minute intervals. However, differences in overpass times between AMSR-E and TMI motivated the calculation of daily averages from the Berg ground data. The AMSR-E data (descending pass) have a local overpass of about 1:30 AM. The TMI data represent daily averages with varying local overpass times due to TRMM's near-equatorial orbit. The author computed daily averages of the ground station measurements, facilitating comparisons among the data sets.

The Berg station is located at 35.0453° N, 97.9167° W. Satellite soil moisture data were obtained from AMSR-E and TMI over the single grid cell representing the study area. Giovanni, a Web-based application developed by the Goddard Earth Sciences Data and Information Services Center, was used to visualize the AMSR-E and TMI soil moisture data. A new Giovanni Soil Moisture instance was developed for this purpose in this study. The bounding box coordinates of the AMSR-E and TMI grid cells which contain the Berg station are listed in Table 7.

Table 11- Satellite Bounding Box Coordinates containing Berg Micronet Station

	West	North	East	South
AMSR-E	-98	35.25	-97.75	35
TMI	-98	35.125	-97.875	35

AERS PGE

As part of this study, the AMSR-E Level-3 Reprojection and Subsetting (AERS) Product Generation Executable (PGE) was developed. The AERS PGE produces a reprojection and subsetting of the Aqua AMSR-E Daily Level 3 Soil Moisture Product. The input AMSR-E HDF files were obtained by the author from the NSIDC. The PGE generates two types of output and associated metadata:

- a netCDF file which contains all **descending** pass soil moisture data from the input AMSR-E Daily Level-3 HDF file
- a tarred file which contains a separate ascii file for each watershed containing subsetting **descending** pass soil moisture data from the input AMSR-E Daily Level HDF file

All output files utilize a 1/4 degree by 1/4 degree cylindrical equidistant grid. The AERS PGE consists of four distinct steps.

The first step is accomplished by hdp, the HDF dumper (<http://hdf.ncsa.uiuc.edu/hdp.html>). This is a command line utility designed for quick display of contents and data of HDF objects. Only the D_Soil_Moisture Scientific Data Set (SDS) is dumped. The output file from hdp contains the descending pass soil moisture data in EASE Grid integer format.

The second step is accomplished by process.exe, a custom executable with source code written in C and compiled using gcc. This step has the effect of replacing the two prior fill values (9999 and -9999) with a single value (-1000). The output file from process.exe contains the descending pass soil moisture data in EASE Grid integer format.

The third step is accomplished by regrid.exe, a custom executable with source code written in C and compiled using gcc. This executable utilizes Mapx, a coordinate

transformation library developed at the NSIDC (<http://geospatialmethods.org/mapx/>).

This executable accepts a bounding box file, the output file from process.exe, a grid parameter definition (gpd) file specifying the input grid and a gpd file specifying the output grid. The input (linux_M1.gpd and M200correct.mpp) and output (linux_cylindrical_equidistant_s01.gpd) gpd files were obtained from the NSIDC [Knowles, 1993]. The interpolation method is nearest-neighbor. The output file from regrid.exe is a single binary file containing the data intended for conversion to netCDF and a separate ascii file for each watershed containing the subsetted soil moisture data.

The fourth step is accomplished using convert2netcdf, a command line executable for converting a file from binary float format to netCDF format which was developed by Denis Nadeau of the GSFC DISC. Convert2netcdf accepts as input the output file from regrid.exe, a Longitude/Latitude bounding box, grid width, and grid height. The data is flipped vertically at this step by specifying 90° and -90° as the southern (SLat) and northern (NLat) limits of latitude, respectively. This step produces a netCDF file which is compatible with Giovanni. As a final step, the PGE generates a metadata file associated with each output file.

The AERS netcdf output files utilize the following filename convention: AMSR_E_L3_DailyLand_B03_YYYYMMDD.nc. The expected file size is ~4.16 MB. The file contains the original AMSR-E data regridded to a 1/4 degree by 1/4 degree cylindrical equidistant grid. The data are not subsetted and contains the entire global range. The file contains three float variables: Longitude, Latitude, and D_Soil_Moisture. The fill value (indicating no valid data) is -1. D_Soil_Moisture is in units of g/cm³.

A separate ascii output file is generated for each watershed. The ascii output files utilize the following filename convention: AMSR_E_YYYY_MM_DD.[WatershedID].txt. Each ascii output file uses a gridded format. Expected file size will vary depending on the size of the bounding box. Each row represents data with the same latitude, and varying longitude. The header at the top of the file includes the watershed ID and its bounding box coordinates. All numbers are floats and utilize constant length fields. Longitude increases towards the right and latitude increases upwards, as is the usual convention. Values of -1.000 indicate grid cells with fill values.

MODIS Processing

Also as part of this study, MODIS data was processed using Matlab. Geolocation (Latitude and Longitude) information was obtained by the author from the MYD03 data product (MODIS Aqua Level 1B Geolocation). The Latitude and Longitude variables each have dimensions of 2030 rows by 1354 columns. The pixel with a minimum distance to the ground station was determined. If more than one 5 minute granule contains the ground site, the pixel with the smaller scan angle was chosen.

The MODIS cannot penetrate clouds, so the cloud mask was needed to remove measurements made under cloudy conditions. The cloud mask was extracted from the MYD021KM and MYD03 products. The pixel closest to the ground station (as determined earlier using the geolocation file) was selected. A cloud mask value of 1 indicates cloudy conditions while a value of 0 indicates clear conditions. Land Surface Temperature was extracted. The pixel closest to the ground station (as determined earlier using the geolocation file) was then selected.

Atmospheric correction was accomplished by the author using software installed at eastfire.gmu.edu/opt/cref. This software was obtained from the NASA GSFC Direct Readout Laboratory. As input, the software requires Level 1B radiance at 250 m, 500 m, and 1 km resolutions (MODIS products MYD02HKM, MYD02QKM, and MYD021KM). As output the software produces atmospheric corrected surface reflectance at 1 km resolution, including Surface Reflectance Bands 1 and 2 (Scientific Data Sets CorrRefl_01 and CorrRefl_02, respectively). Values for each band were obtained by the author for the selected pixel, scaled to scientific units (with a scale factor of $1.0E-4$), and used to calculate NDVI. Land Surface Temperature (LST) was obtained by the author directly from the MYD11_L2 product.

RESULTS

Time Series graphs for the grid cells described in the Methodology section were generated using Giovanni for part of the crop-covered season (June, July, and August). The time series for the AMSR-E and TMI satellite data and the Berg ground data for June, July, and August 2003 are shown in Figure 5, Figure 6, and Figure 7, respectively. In order to facilitate understanding the relationship between soil moisture satellite measurement and significant rainfall events, Daily TRMM (3B42 V6 derived) precipitation data are also plotted using the secondary y axis.

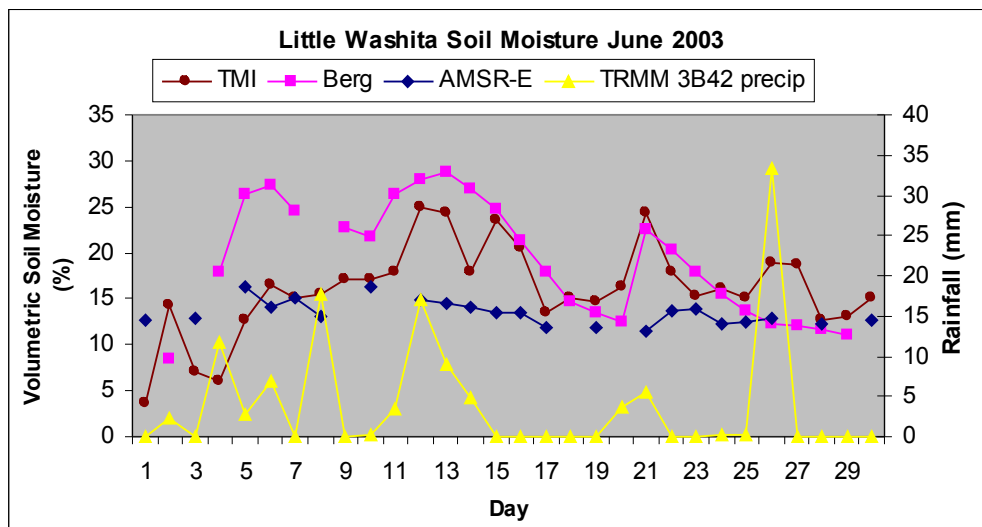


Figure 5- Little Washita Soil Moisture June 2003

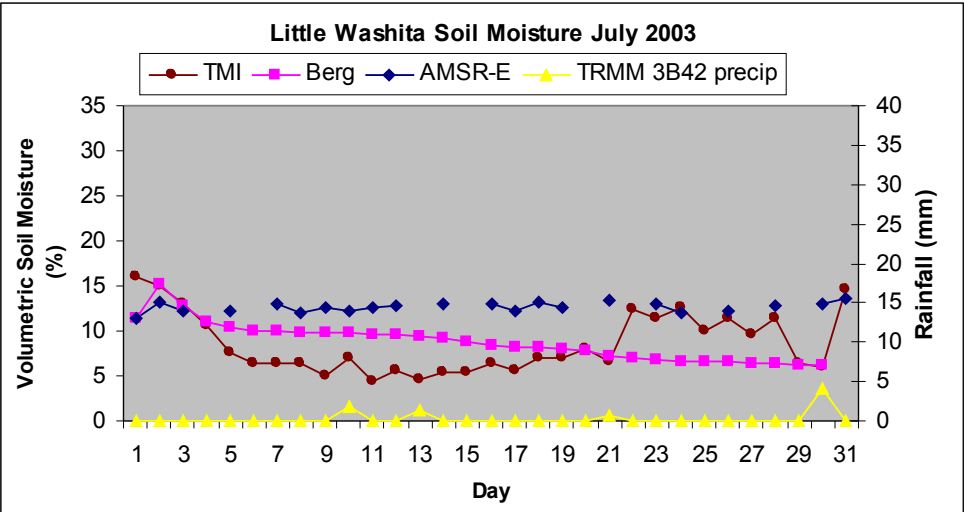


Figure 6- Little Washita Soil Moisture July 2003

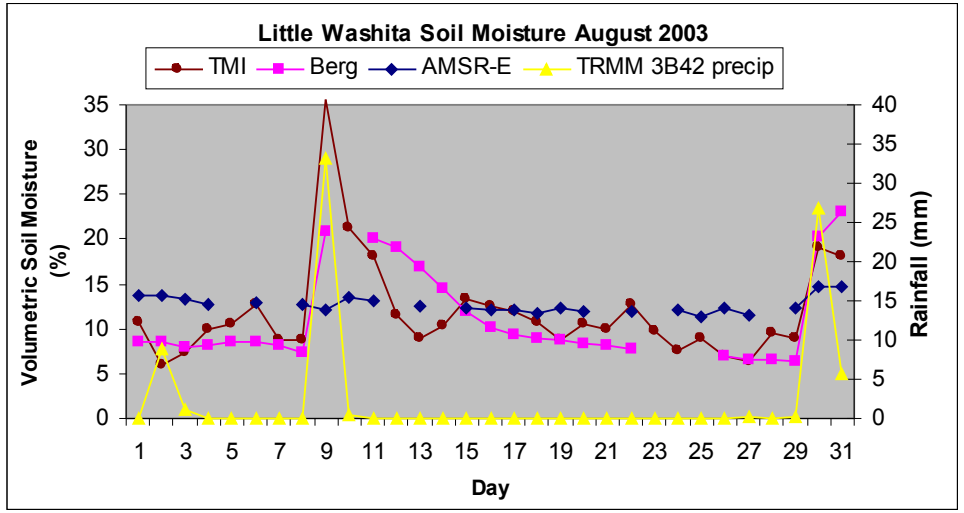


Figure 7- Little Washita Soil Moisture August 2003

The correlation coefficients between AMSR-E soil moisture and the in-situ measurements and between TMI and the in-situ measurements at LWREW were calculated for each month and are shown in Table 12. Similarly, the correlation coefficients between TMI soil moisture and the in-situ measurements are shown in Table 13.

Table 12- Correlation between AMSR-E soil moisture and in-situ measurements at LWREW in 2003

Month	R ²
June	.4273
July	.0155
August	.2646
June-August (crop-covered)	.3709

Table 13- Correlation between TMI soil moisture and in-situ measurements at LWREW in 2003

Month	R ²
June	.2203
July	.0393
August	.4937
June-August (crop-covered)	.5153

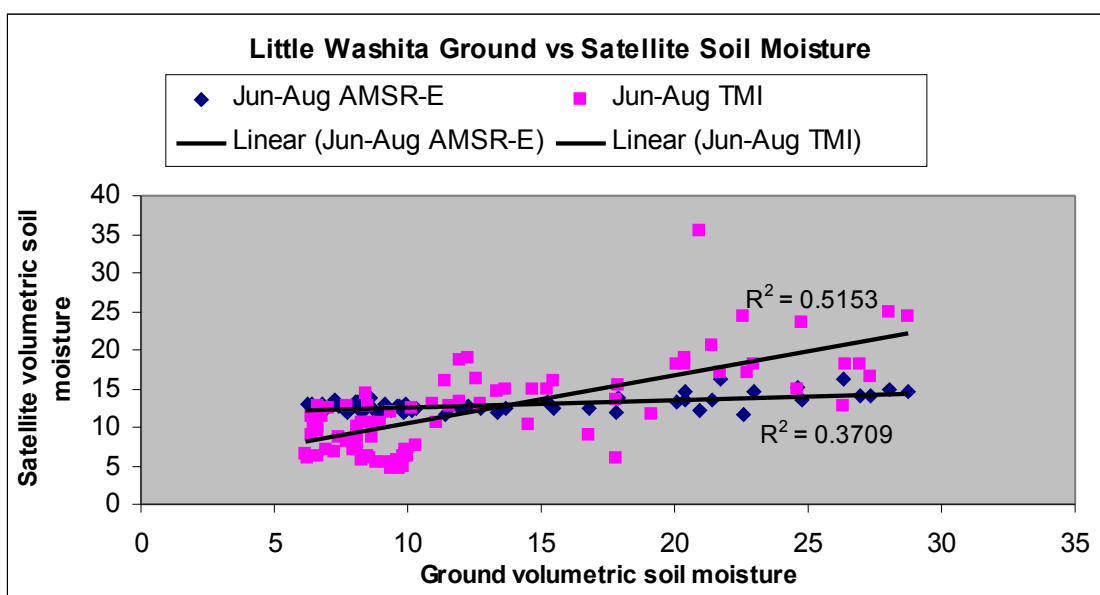


Figure 8- Little Washita Ground and Satellite Soil Moisture, June-August 2003

Time Series graphs for the grid cells described in the Methodology section were generated using Giovanni for part of the crop-covered season (June, July, and August) as well as part of the non-crop-covered season (December, January, and February). The time series for the AMSR-E and TMI satellite data and the SCAN ground data for June, July, and August 2003 are shown in Figure 9, Figure 10, and Figure 11, respectively.

The time series for the AMSR-E and TMI satellite data and the SCAN ground data for December, January, and February 2003 are shown in Figure 12, Figure 13, and Figure 14, respectively. Daily TRMM (3B42) precipitation data are also plotted.

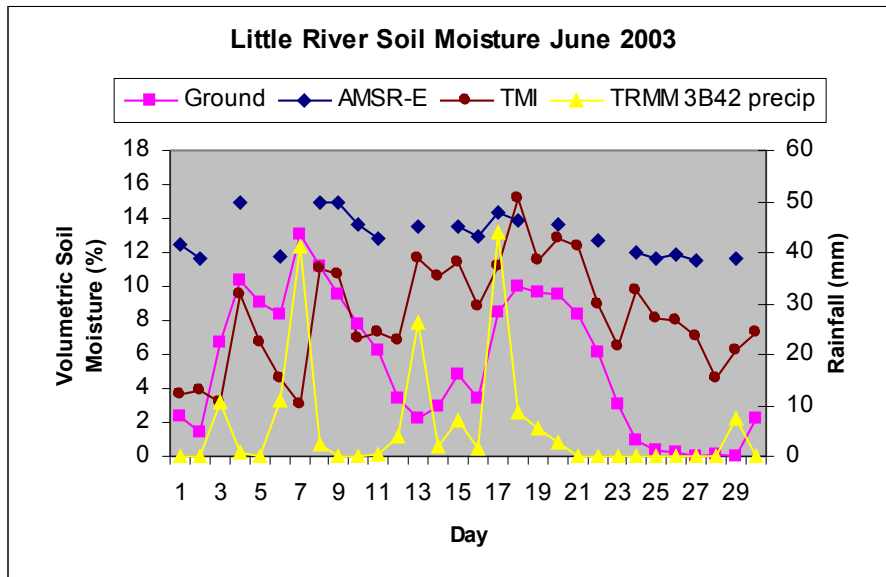


Figure 9- Little River Soil Moisture June 2003

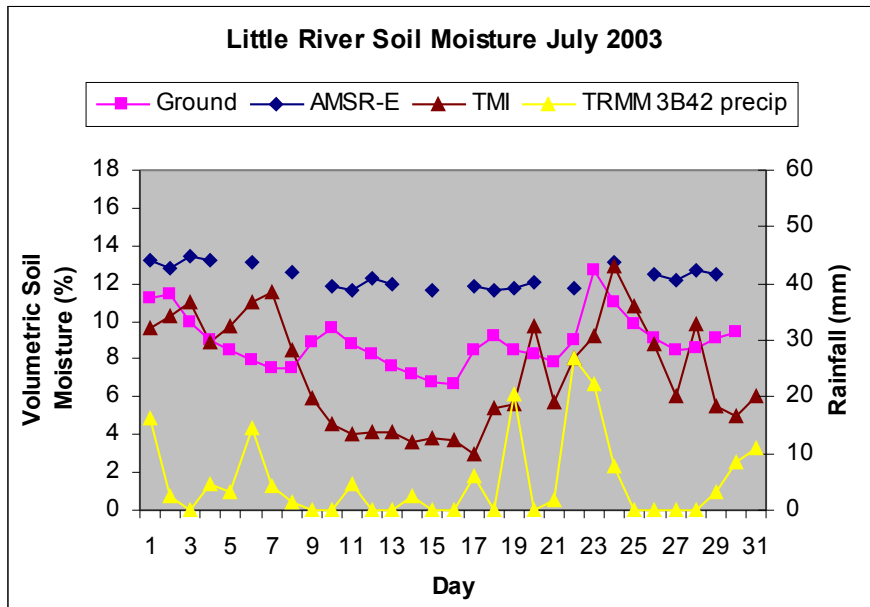


Figure 10- Little River Soil Moisture July 2003

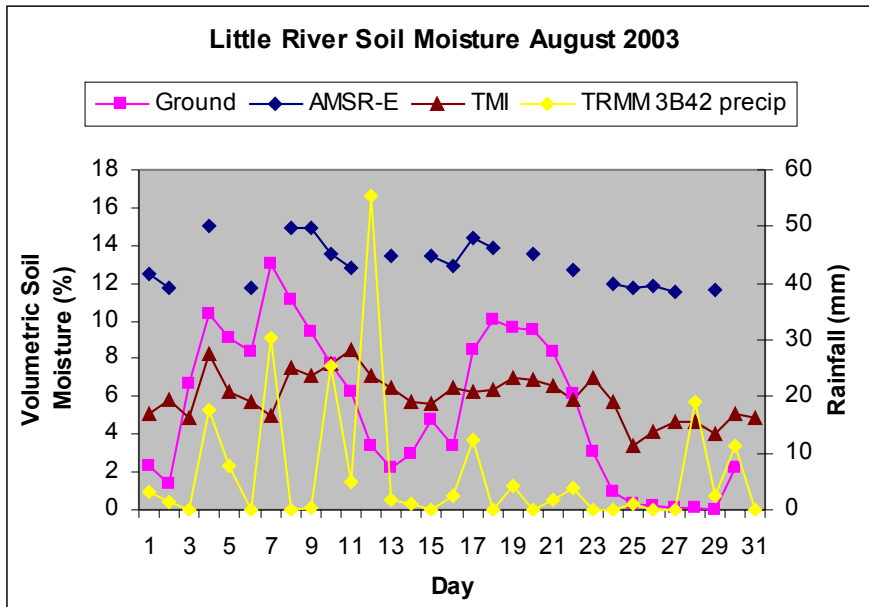


Figure 11- Little River Soil Moisture August 2003

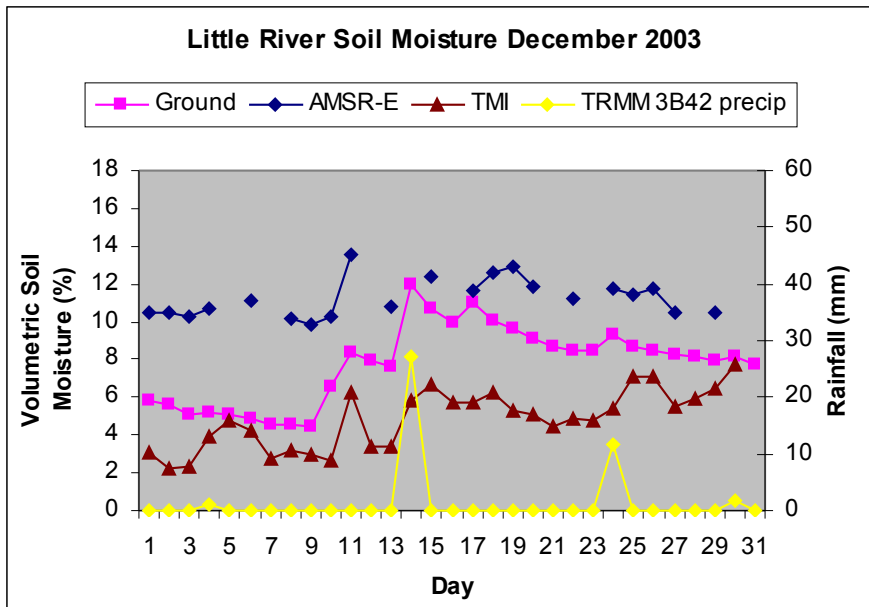


Figure 12- Little River Soil Moisture December 2003

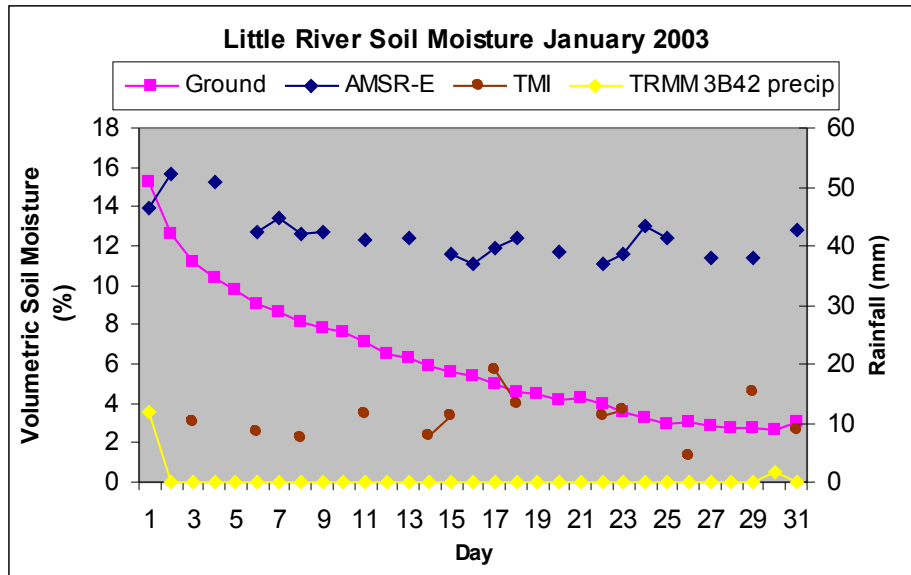


Figure 13- Little River Soil Moisture January 2003

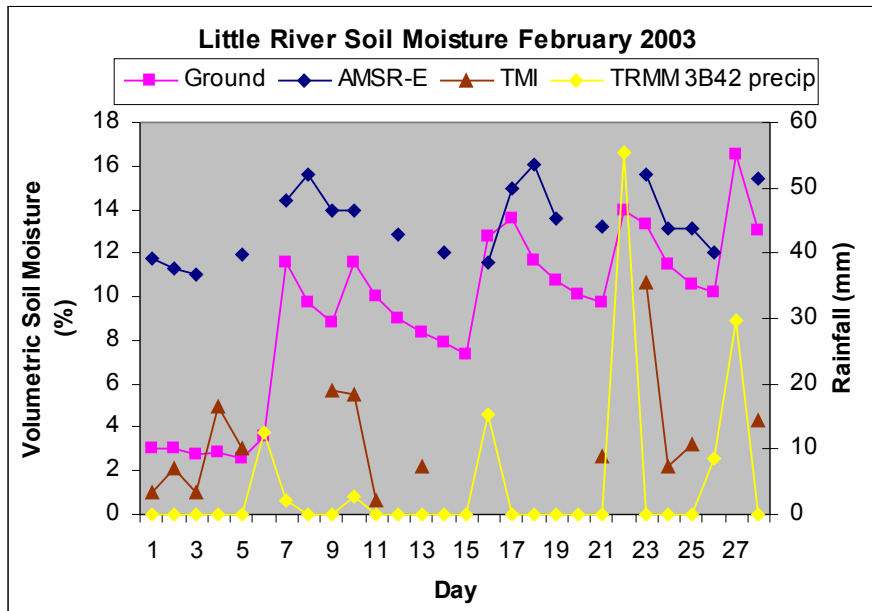


Figure 14- Little River Soil Moisture February 2003

The correlation coefficients between AMSR-E and the in-situ measurements as well as TMI and the in-situ measurements at LREW were calculated for each month and are shown in Table 14. Similarly, the correlation coefficients between TMI soil moisture and the in-situ measurements are shown in Table 15.

Table 14- Correlation between AMSR-E soil moisture and in-situ measurements at LREW in 2003

Month	R²
June	.6769
July	.2466
August	.3231
December	.5209
January	.5552
February	.4799
June – August (crop-covered)	.1801
December – February (non-crop-covered)	.4086

Table 15- Correlation between TMI soil moisture and in-situ measurements at LREW in 2003

Month	R²
June	.0851
July	.1865
August	.2015
December	.4887
January (13 days)	.0442
February (14 days)	.2116
June – August (crop-covered)	.0113
December – February (non-crop-covered)	.2198

Overall, the correlation with ground measurements was much better for AMSR-E than TMI over this study area for all months. The AMSR-E soil moisture observations correlated particularly well with ground measurements during the non-crop covered period of December through February with an overall correlation coefficient of 0.4086 despite the occurrence of snowfall during this period.

MODIS geolocation information was used to determine the pixel closest to the Berg ground station within the LREW. Data was processed for June 1, 2003 through

August 31, 2003, representing the crop-covered season. Daily valid data requires a cloud mask of zero (indicating clear conditions) and a non-zero LST. Days with measured ground soil moisture values over 25 are also excluded. These conditions are described in . These criteria resulted in 21 valid points for June 1 – August 31 of 2003. LST, NDVI, and measured soil moisture (Sm) were obtained for these points.

Table 16- Criteria for valid MODIS daily data

Measurement	Condition
Cloud Mask	0, indicating clear conditions
Land surface temperature	≠ 0, indicating valid data
Average daily measured soil moisture at ground station	< 25

A regression analysis was performed using the following equation [Wang *et al*, 2007]:

$$Sm = a_0 + a_1 * NDVI + a_2 * LST + a_3 * NDVI * LST + a_4 * NDVI^2 + a_5 * LST^2 \quad (3)$$

Results are shown in Figure 15. R² is fairly high. The standard error is 2.7038. The P-value is close to zero.

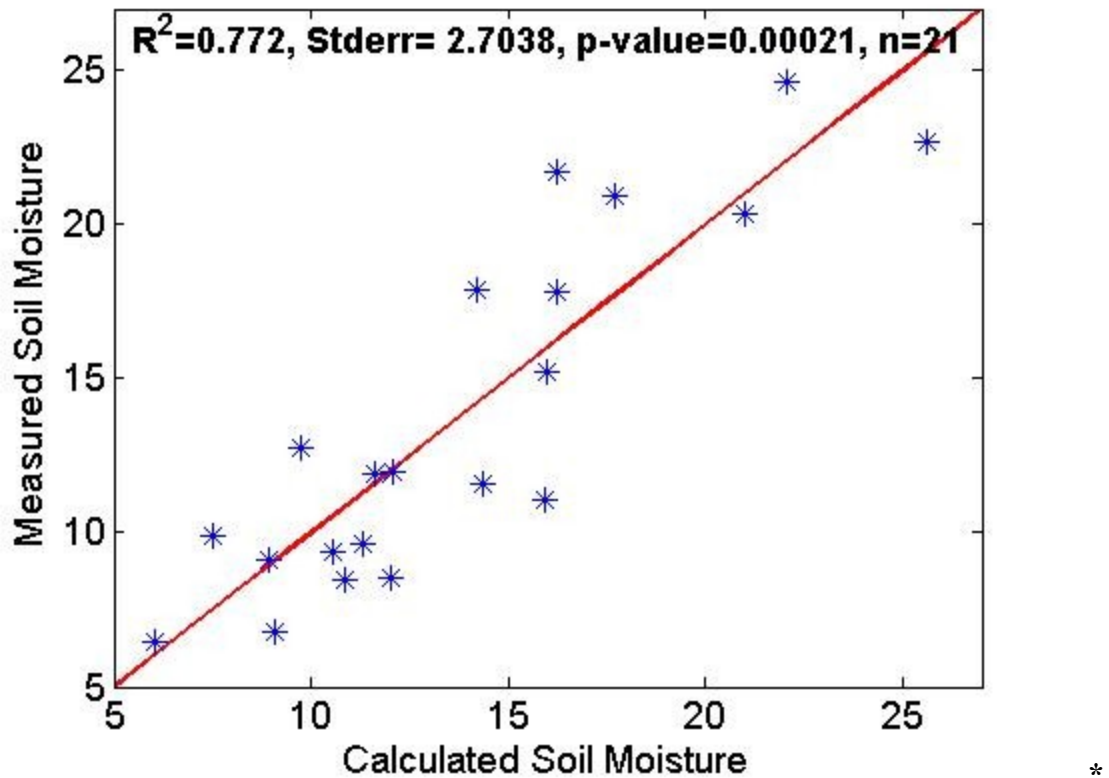


Figure 15- Correlation of Calculated Soil Moisture using MODIS Data with Measured Soil Moisture for June – August of 2003

Satellite retrieval of soil moisture by definition represents an average of the values found over the footprint area. For this reason, satellite retrieval of soil moisture is best accomplished over homogenous surfaces with a single vegetation type and areas with significant variability in topography, land cover, or vegetation type over a single grid cell will present increased retrieval errors. Consistent precipitation patterns throughout the study area also facilitate satellite measurement.

A major limitation of current microwave satellite measurements is the coarse spatial resolution available. Each AMSR-E grid cell is $1/4^\circ$ by $1/4^\circ$ (~25 km by 25 km) and each TMI grid cell is $1/8^\circ$ by $1/8^\circ$. MODIS grid cells have a minimum spatial

resolution of 1 km by 1 km. In situ data, such as that from the ARS Micronet and SCAN stations, is measured at a single point with infinitesimally small area. In addition, emissivity is representative of the average soil moisture in the soil up to depth d . For AMSR-E, we can show that $d < 2$ mm [Njoku, 1999]. Therefore AMSR-E soil moisture retrievals approximate skin soil moisture while the ARS Micronet and SCAN stations utilize sampling depths of about 5 cm (at shallowest). It is difficult to compare two inherently different methods of measurement such as satellite retrieval and in-situ measurement. These differences undoubtedly introduce error.

As discussed in the Theoretical Description of Microwave Soil Moisture Retrieval, current microwave satellite retrieval algorithms are limited to areas of low or moderate vegetation (with water content of less than 5 kg/m²). Vegetation increases scattering and therefore measurements may become unreliable in areas of high or variable vegetation. These effects were minimized by conducting this study in two areas where the vegetation patterns are well-known. Also, the presence of clouds and precipitation causes unexpected effects that are not modeled in the retrieval algorithm.

As emissivity is a function of the satellite's incidence angle (θ), the equivalent microwave temperature measured by the sensor depends on the nature of its antenna pattern. Radiation collected in the antenna sidelobes can incorrectly be interpreted as radiation in the main lobe [Elachi and van Zyl, 2006]. Main beam efficiencies have been calculated to quantify the measurement ambiguity. The 6.9 and 10.6 GHz bands have efficiencies of 95.3% and 95% respectively; error due to the antenna sidelobes is low [Njoku, 2004].

RFI also proved to be a major issue in AMSR-E measurements, even motivating a change in Njoku's Level 3 soil moisture retrieval algorithm [*Njoku and Chan, 2005*]. RFI sources at L-Band and mitigations strategies are areas of current research for SMAP [*SMAPVEX08 Experiment Plan, 2008*]. These areas must be studied further and mitigation techniques must be applied in order to obtain meaningful satellite soil moisture measurements.

CONCLUSION AND DISCUSSION

Overall, the AMSR-E soil moisture data exhibited a smaller range of variability than the TMI data. This can be seen in Figure 5, Figure 6, and Figure 7. For example, during the time period of June, July, and August of 2003 (representing the crop-covered season), the standard deviations of the AMSR-E, TMI, and in-situ measurements over the Little Washita study area were 1.02, 5.63, and 6.49, respectively. During this time period, TMI measurements correlated better with the in-situ measurements ($R^2 = 0.5153$) than the AMSR-E measurements did ($R^2 = 0.3709$).

The TRMM 3B42 rainfall data shows significant precipitation events in June and August of 2003 over the Little Washita study area, including June 12, June 21, June 26, August 9, and August 30. These precipitation events are reflected in the in-situ and TMI soil moisture measurements but not in the AMSR-E soil moisture measurements. One factor may be the lower spatial resolution of AMSR-E ($1/4^\circ$ vs $1/8^\circ$). In July of 2003, the correlation coefficients of both AMSR-E and TMI with the in-situ data were low. However, almost no significant rainfall occurred in this month, as indicated by the TRMM 3B42 data and the steadily decreasing in-situ measurements in Figure 6. This may indicate a minimum threshold of soil moisture desired for accurate satellite measurements.

The AMSR-E soil moisture data over the Little Washita study area exhibited a smaller range of variability than the TMI or the in-situ data, as seen in Figure 5 - Figure 7. During the time period of June, July, and August of 2003 (representing the crop-covered season), the standard deviations of the AMSR-E, TMI, and in-situ measurements over the Little Washita study area were 1.01, 5.63, and 6.59, respectively. Similarly, during the crop-covered season the standard deviations of the AMSR-E, TMI, and in-situ measurements over the Little River study area were 0.818, 2.70, and 3.09, respectively. Also, the AMSR-E retrievals obtained using Njoku's algorithm exhibited a positive bias with respect to the Berg ground measurements. In an AMSR-E Soil Moisture Algorithm Validation Exercise over Little Washita using data from June 18, 2002 through December 31, 2005, Jackson also found that AMSR-E soil moisture retrievals obtained using the Njoku algorithm exhibited a smaller range of variability and positive bias when compared to in-situ measurements [Jackson, Cosh, and Zhan, 2006]. In a study comparing REMEDHUS in-situ measurements to four satellite soil moisture datasets over Spain from January 1, 2003 through December 31, 2005, Wagner found that the AMSR-E Njoku product was characterized by low variability of soil moisture [Wagner *et al*, 2006].

Significant precipitation events in June, July, and August of 2003 over the Little River study site can be seen in the TRMM 3B42 data plotted in Figure 9, Figure 10, and Figure 11. These events are reflected also in the in-situ and TMI soil moisture measurements, at times with a delay. For example, a significant precipitation event on June 17 is followed by a spike in soil moisture on June 18 in both the in-situ and TMI data. Another example occurs on July 22, followed by spikes in soil moisture

measurements on July 24 in the in-situ and TMI data. During the crop-covered season neither AMSR-E ($R^2 = 0.1801$) nor TMI ($R^2 = 0.0113$) measurements correlated well with the in-situ measurements. This may be due to the presence of moderate to high vegetation in the Little River study area, which is 31% row crops but also 50% woodland. As discussed earlier, current microwave satellite retrieval algorithms are limited to areas of low or moderate vegetation.

In the non-crop-covered season (represented by December, January, and February of 2003) the standard deviations of the AMSR-E, TMI, and in-situ measurements over the Little River study area were 1.54, 3.35, and 1.92 respectively. During this time period, AMSR-E measurements exhibit a range of variability comparable to that of the in-situ measurements. AMSR-E correlated fairly well with ground measurements in December, January, and February, with correlation coefficients of 0.5209, 0.5552, and 0.4799, respectively. These AMSR-E results are far better than those obtained during the crop-covered season at the Little River site, indicating that AMSR-E may perform well in study areas that contain mostly bare soil or low vegetation.

As seen in Figure 13 and Figure 14, about half of the daily TMI soil moisture data in January and February of 2003 was masked out. The TMI data utilizes precipitation, vegetations sensitivity, and snow cover, frozen soil, and surface water masks to remove data that is likely to have low accuracy. In January and February of 2003, only 13 and 14 days of valid data (respectively) were obtained. In both cases this is less than half of the month. The exact conditions that caused one of the masks to be used are unknown.

However, these conditions may have contributed to the low correlation between the TMI and in-situ measurements during the non-crop-covered season.

The Little Washita area was also analyzed in this study using MODIS Level 1B data. Criteria were used to determine whether daily data were “good,” including a cloud mask of zero, a non-zero land surface temperature, and average daily measured soil moisture of less than 25 (% volumetric). Data that did not fit strict criteria were not considered. Application of the criteria resulted in 21 valid points between June 1 and August 31 of 2003. A linear regression was applied to relate Land Surface Temperature, NDVI, and measured soil moisture. The results shown in Figure 15 were obtained. Therefore the MODIS data correlated best with the in-situ data, with a correlation coefficient of 0.772.

In conclusion, during the crop-covered season of June, July, and August of 2003 at Little Washita River Experimental Watershed, the optical MODIS soil moisture retrievals correlated better with ground measurements than the microwave AMSR-E or TMI retrievals. The spatial resolution of MODIS (1 km) is finer than the spatial resolution of AMSR-E (~25 km) or TMI. Spatial resolution is an important factor because topography, soil properties, and vegetation cover may vary significantly over satellite footprints. Both microwave sensors are limited by their coarse spatial resolution. However, optical measurements are limited to cloud-free conditions. Future work includes research on algorithms which combine optical and microwave measurements to provide the advantages of each. Other future work includes analysis of Owe and de Jeu’s new global surface soil moisture dataset, which is derived using all available historical

and active satellite microwave sensors [*Owe et al*, 2008], and comparison with SMEX03 field campaign data. Also, an automated system providing MODIS soil moisture retrievals for any spatial or temporal subset would facilitate analysis of MODIS soil moisture over additional study sites and time periods.

REFERENCES

REFERENCES

- Allen, P.B. and J.W. Nancy (1991). Hydrology of the Little Washita Watershed, Oklahoma: Data and Analyses. U.S. Department of Agriculture, Agricultural Research Service, ARS-90.
- Anderson, M.G. and P.D. Bates (2001). Hydrological Science: Model Credibility and Scientific Integrity in *Model Validation: Perspectives in Hydrological Science*. John Wiley & Sons, Chichester, England, 1-10.
- Ashman, M. and G. Puri (2002). *Essential Soil Science: A Clear and Concise Introduction to Soil Science*, 208 pp., Blackwell Science, Oxford and Malden, MA.
- Bailey, R.J. and E. Spackman (2007). A model for estimating soil moisture changes as an aid to irrigation scheduling and crop water-use studies. *Soil Use and Management*, 12(3), 122-128.
- Brady, Nyle C (1974). *The Nature and Properties of Soils*, 8th ed., 639 pp., Macmillan Publishing Co, Inc, New York, NY.
- Brodzik, M. J. and K. W. Knowles (2002). "EASE-Grid: a versatile set of equal-area projections and grids" in M. Goodchild (ed.) *Discrete Global Grids*. Santa Barbara, CA: National Center for Geographic Information and Analysis.
- Carlson, T., Gillies, R. and Perry, E. (1994). A method to make use of thermal infrared temperature and NDVI measurements to infer surface soil water content and fractional vegetation cover. *Remote Sensing Reviews*, 9, 161-173.
- Chauhan, N.S., S. Miller, and P. Ardanuy (2003). Spaceborne soil moisture estimation at high resolution: a microwave-optical/IR synergistic approach. *International Journal of Remote Sensing*, 24(22), 4599-4622.
- Cosh, M. H., T. J. Jackson, P. Starks, G. Heathman (2006). Temporal Stability of surface soil moisture in the Little Washita River watershed and its applications in satellite soil moisture product validation. *Journal of Hydrology*: 323, 168-177.

Dai, Aiguo, Kevin E. Trenberth, and Taotao Qian (2004). A Global Dataset of Palmer Drought Severity Index for 1870-2002: Relationship with Soil Moisture and Effects of Surface Warming. *Journal of Hydrometeorology*, 5, 1117-1130.

De Jeu, R. and M. Owe (2003). Further validation of a new methodology for surface moisture and vegetation optical depth retrieval. *International Journal of Remote Sensing*, 24:4559-4578.

Doraiswamy, P. C., J. L. Hatfield, T. J. Jackson, B. Akhmedov, J. Prueger, and A. Stern (2004). Crop condition and yield simulations using Landsat and MODIS. *Remote Sensing of Environment*, 92(4), 548-559.

Dzurik (2003). *Water Resources Planning*, 3rd ed., 392 pp., Rowman and Littlefield Publishers, Inc, Lanham, Maryland.

Elachi, C. and J. Van Zyl (2006). *Introduction to the Physics and Techniques of Remote Sensing*, 2nd ed., 552 pp., John Wiley & Sons, Hoboken, New Jersey.

Elliott, R.L., F.R. Schiebe, K.C. Crawford, K.D. Peter and W.E. Puckett (1993). A Unique Data Capability for Natural Resources Studies. Paper No. 932529, International Winter Meeting; American Society of Agricultural Engineers, Chicago, IL, Dec. 14-17.

Gao, H., Wood, E. F., Jackson, T. J., Drusch, M., and Bindlish, R. (2006). Using TRMM/TMI to retrieve surface soil moisture over the southern United States from 1998 to 2002. *J. Hydrometeorology*, 7(1), 23-38, doi: 10.1175/JHM473.1

Gillies, R. R., W. P. Kustas, and K. S. Humes (1997). A verification of the 'triangle' method for obtaining surface soil water content and energy fluxes from remote measurements of the normalized difference vegetation index (NDVI) and surface radiant temperature. *International Journal of Remote Sensing*, 18(15), 3145-3166.

Griffin, Michael (2006). *The Future of NPOESS: Results of the Nunn-McCurdy Review of NOAA's Weather Satellite Program*. House Science Committee Hearing, June 8.

Grody, N., F. Weng, and R. Ferraro (2000). Application of AMSU for obtaining hydrological parameters in P. Pampaloni and S. Paloscia (eds), *Microwave Radiometry and Remote Sensing of the Earth's Surface and Atmosphere*, VSP Publications, The Netherlands, 339-351.

Hao, X., J. Qu, S. Zhang, L. Wang, and S. Dasgupta (2006). An Integrated System for Soil Moisture Retrieval with Satellite Remote Sensing. 36th COSPAR Scientific Assembly, July 16-23, Beijing, China.

Huang, Jin, Huug M. van den Dool, and Konstantine P. Georgarakos (1996). Analysis of Model-Calculated Soil Moisture over the United States (1931-1993) and Applications to Long-Range Temperature Forecasts. *Journal of Climate*, 9(6), 1350-1362.

Illston, B.G., J.B. Basara, D K. Fisher, R. Ellitt, C.A. Fiebrich, K.C. Crawford, K. Humes, and E. Hunt (2008). Mesoscale Monitoring of Soil Moisture across a Statewide Network. *American Meteorological Society*, 25, 167-182.

Jackson, T., M. H. Cosh, X. Zhan, D. Bosch, M. Seyfried, P. Starks, T. Keefer, and V. Lakshmi (2006). Validation of AMSR-E Soil Moisture Products Using Watershed Networks. Proceedings of the International Geoscience and Remote Sensing Symposium Proceedings, July 31-August 4, 2006, Denver, Colorado, 432-435.

Jackson, T., M. Cosh, and X. Zhan (2006). Update on Validation of Satellite Soil Moisture Algorithms Using Watershed Networks. Joint AMSR Science Team Meeting, September 6-8, 2006, La Jolla, California.

Jackson, T. J., and T. J. Schmugge (1991). Vegetation Effects on the Microwave Emission of Soils. *Remote Sensing of the Environment*, 36, 203-212.

Knowles, K. W. (1993). Points, pixels, grids, and cells: A Mapping and Gridding Primer. Unpublished report. Boulder CO: National Snow and Ice Data Center.

Lal, Rattan and Monoj K. Shukla (2004). *Principles of Soil Physics*, 528 pp., Marcel Dekker, Inc, New York, New York.

Li, L, E. G. Njoku, E. Im, P. Chang and K. St. Germain (2004). A preliminary survey of radio-frequency interference over the U.S. in Aqua AMSR-E data. *IEEE Trans. Geosci. Remote Sens.*, 42(2), 380-390.

Martin-Neira, M (1997). MIRAS- A Two-Dimensional Aperture-Synthesis Radiometer for Soil Moisture and Ocean Salinity Observations. European Space Agency Bulletin 32, November 1997.

McCabe, M. F., H. Gao, and E. F. Wood (2005). Evaluation of AMSR-E-Derived Soil Moisture Retrievals Using Ground-Based and PSR Airborne Data during SMEX02. *Journal of Hydrometeorology*, 6(6), 864-877.

McCabe, M. F., E. F. Wood, and H. Gao (2005). Initial soil moisture retrievals from AMSR-E: Multiscale comparison using in situ data and rainfall patterns over Iowa, *Geophysical Research Letters*, 32(L06403).

Merz, Bruno and Erich J. Plate (1997). An Analysis of the Effects of Spatial Variability of Soil and Soil Moisture on Runoff. *Water Resources Research*, 33(12), 2909-2922.

- NASA/NOAA (2007). Impacts of NPOESS Nunn-McCurdy Certification on Joint NASA/NOAA Climate Goals. Originally presented to the Office of Science and Technology Policy on January 8, 1007. Updated April 24, 2007
- Njoku, E. G. (1999). AMSR Land Surface Parameters, Algorithm Theoretical Basis Document, version 3, Jet Propulsion Laboratory, California Institute of Technology, Pasadena, California.
- E. Njoku, T. Koike, T. Jackson, and S. Paloscia (2000). "Retrieval of soil moisture from AMSR data," in P. Pampaloni and S. Paloscia (eds), *Microwave Radiometry and Remote Sensing of the Earth's Surface and Atmosphere*, VSP Publications, The Netherlands, 525-533.
- Njoku, E. G., Jackson, T. J., Lakshmi, V., Chan, T.K., Nghiem, S.V. (2003). Soil moisture retrieval from AMSR-E. *Geoscience and Remote Sensing, IEEE Transactions on* , 41(2), 215-229.
- Njoku, E. G. (2004) updated daily. AMSR-E/Aqua Daily L3 Surface Soil Moisture, Interpretive Params, and QC EASE-Grids, March to June 2004. Boulder, CO: National Snow and Ice Data Center.
- Njoku, E.G., P. Ashcroft, T.K. Chan and L. Li (2005). Global survey and statistics of radio-frequency interference in AMSR-E land observations. *IEEE Trans. Geosci. Remote Sens.*, 43(5), 938-947.
- Njoku, E. G. and Steven Chan (2005). Vegetation and surface roughness effects on AMSR-E land observations. *Remote Sensing of Environment*, 100(2): 190-199.
- Oklahoma Ag in the Classroom (2008). *Oklahoma Crop Calendar*. <http://agweb.okstate.edu/fourh/aitc/calendar/cropcal.html>
- Owe, M., R. de Jeu, and J. Walker (2001). A methodology for surface soil moisture and vegetation optical depth retrieval using the microwave polarization difference index. *Geoscience and Remote Sensing, IEEE Transactions on* , 39(8) 1643-1654.
- Owe, M., R. de Jeu, and T. Holmes (2008). Multisensor historical climatology of satellite-derived global land surface temperature. *Journal of Geophysical Research*, 113, F01002.
- Schaetzl, Randall and Sharon Anderson (2005). *Soils: Genesis and Geomorphology*, 817 pp., Cambridge University Press, Cambridge, UK.

Soil Moisture Active Passive (SMAP) Mission NASA Workshop Report, July 9-10, 2007.

http://nasascience.nasa.gov/msrd/earth-science/decadal-surveys/Volz1_SMAP_11-20-07.pdf

Soil Moisture Active Passive Validation Experiment 2008 (SMAPVEX08) Experiment Plan. Version September 4, 2008.

ftp://hydrolab.arsusda.gov/pub/tjackson/SMAPVEX08/SMAPVEX08_EP_090408.pdf

Soil Moisture and Ocean Salinity (SMOS) Mission Objectives and Scientific Requirements, (2002) ESA.

http://esamultimedia.esa.int/docs/SMOS_MRD_V5.pdf

Soil Survey Division Staff (1993). *Soil Survey Manual*. Soil Conservation Service. U.S. Department of Agriculture Handbook 18.

Southeast Regional Climate Center (1997). *Growing Season Summary*.

<http://climate.engr.uga.edu/tifton/growing.html>

Stevens Water Monitoring Systems, Inc. Hydra Probe II Soil Sensor Data Sheet.

Portland, Oregon. http://www.stevenswater.com/catalog/products/soil_sensors/datasheet/hydraprobeiidatasheetnewweb.pdf

Teng, W. L, J. R. Wang, and P.C. Doraiswamy (1993). Relationship between satellite microwave radiometric data, antecedent precipitation index, and regional soil moisture. *International Journal of Remote Sensing*, 14(13), 2483-2500.

Vall-llossera, M., Cardona, M., Blanch, S., Camps, A., Monerris, A., Corbella, I., Torres, F., Duffo, N (2005). L-Band Dielectric Properties of Different Soil Types Collected during the MOUSE 2004 Field Experiment. *Proceedings of International Geoscience and Remote Sensing Symposium*, Seoul, Korea, July 2005.

Wagner, W., Naeimi, V., Scipal, K., de Jeu, R., Martinez-Fernandez, J (2006). Soil moisture from operational meteorological satellites. *Hydrogeology Journal*, 15(1), 121-131.

Wang, L, J.J. Qu, S, Zhang, X. Hao, and S. Dasgupta (2007). Soil moisture estimation using MODIS and ground measurements in eastern China. *International Journal of Remote Sensing*, 28(6), 1413-1418.

Weltz, M. A. and D. A. Bucks (2003). *The USDA-Agricultural Research Service Watershed Research Program*. First Interagency Conference on Research in the Watersheds, October 27-30, 2003. U.S. Department of Agriculture, Agricultural Research Service.

Zhan, X., S. Miller, N. Chauhan, L. Di, P. Ardanuy (2002). Soil Moisture Visible/Infrared Imager/Radiometer Suite Algorithm Theoretical Basis Document, Version 5. Raytheon Systems Company, Lanham, MD, March 2002.

CURRICULUM VITAE

Melissa Soriano graduated from Thomas Jefferson High School for Science and Technology in 1999. She received her Bachelors of Science from the California Institute of Technology in 2003, double majoring in Electrical and Computer Engineering and Business Economics and Management. She researched soil moisture as a graduate research assistant for the Goddard Space Flight Center Data and Information Services Center in 2007 and 2008. Melissa is a member of the Tracking Systems and Applications Section at the Jet Propulsion Laboratory, which is operated by the California Institute of Technology for NASA. She is also a member of the EastFIRE Laboratory at George Mason University.